Study on methods of suppression of cell aggregation and utilization of pigs as cell source in mesenchymal stem cell therapy

April 2024

Takeshi Kikuchi

Table of contents

1. Abstract 3
2. General introduction 5
3. Avoiding aggregation of human bone marrow–derived mesenchymal stem cells stored in cell preservation solutions 13
3.1 Introduction 13
3.2 Materials and methods 14
3.3 Results 18
3.4 Discussion 22
3.5 Conclusions 23
4. Relationship between oxygen partial pressure and inhibition of cell aggregation of human adipose tissue-derived mesenchymal stem cells stored in cell preservation solutions 24
4.1 Introduction 24
4.2 Materials and methods 26
4.3 Results 31
4.4 Discussion 38
4.5 Conclusions 41
5. Development and characterization of islet-derived mesenchymal stem cells from clinical grade neonatal porcine cryopreserved islets 42
5.1 Introduction 42
5.2 Materials and methods 44
5.3 Results 53
5.4 Discussion 62

5.5 Conclusions.....67
6. Development and characterization of Gal KO porcine bone marrow-derived mesenchymal stem cells.....68
6.1 Introduction.....68
6.2 Materials and methods.....69
6.3 Results.....79
6.4 Discussion.....88
6.5 Conclusions.....90
7. Overall conclusion.....91
8. Acknowledgment.....97
9. Reference.....98

1. Abstract

To further develop mesenchymal stem cell (MSC) therapy, ensuring safety during MSC administration and a reliable source of donor cells are necessary. In this study, we investigated the conditions under which aggregation occurs during MSC preservation and those that suppress aggregation in order to minimize the risk of embolization during intravascular administration of MSCs. We also focused on pigs as a stable source of MSCs. We developed a method for isolating MSCs from clinical-grade pigs kept under infection control protocols or Gal antigen knockout (KO) produced by genome editing to suppress rejection. We also studied the development of MSCs from cryopreserved tissues, as cryopreservation of derived tissues is useful for the stable supply of MSCs. The isolated MSCs were then characterized to evaluate the possibility of using pigs as a donor source.

Preservation of human bone marrow-derived MSCs (hBM-MSCs) and human adipose tissue-derived MSCs (hADSCs) in lactated Ringer's solution with 3% trehalose and 5% dextran 40 (LR-3T-5D) for 24 h at 25 °C resulted in higher cell viability than cells preserved in lactated Ringer's solution. However, cell aggregation occurred under the 25 °C storage condition with LR-3T-5D. These aggregations could be suppressed by preservation at 4 °C. Furthermore, assuming a situation where cells are administered slowly at room temperature, we investigated conditions that would inhibit aggregation even with storage at 25 °C. In the study using hBM-MSCs, aggregation was suppressed by extending the trypsin treatment time from 5 to 10 min at the time of cell collection. When hADCSs were assessed under the same conditions, this aggregation could be suppressed by decreasing the partial oxygen pressure (pO_2) in the solution through increasing the volume of preservation solution, increasing the cell concentration, and

replacing the headspace of the preservation container with nitrogen gas. Thus, there is a relationship between cell aggregation and pO_2 in preservation solutions.

MSCs could be established using islets cryopreserved for more than 4 years from clinical-grade neonatal pigs (clinical-grade npISLET-MSCs). The diameter of the clinical-grade npISLET-MSCs was larger than that of non-clinical-grade neonatal pig-derived bone marrow MSCs, and the clinical-grade npISLET-MSCs proliferated at a slower rate. Compared to MSCs established from non-clinical-grade neonatal porcine islets, no differences in proliferation, cell size, and surface markers were observed. MSCs were established from bone marrow of Gal-KO adult pigs (Gal-KO apBM-MSCs) and compared to MSCs established from wild-type adult pig bone marrow (WT apBM-MSCs). Gal-KO apBM-MSCs showed reduced Gal expression. The colony-formation efficiency of Gal-KO apBM-MSCs was approximately one-half that of WT apBM-MSCs. However, no significant differences in differentiation ability, MSC surface markers, and proliferation were observed. The expression levels of angiogenesis-related genes (*VEGFA*, *IGF1*, *ADM*) and immunosuppression-related genes (*IDO1*, *PTGES*, *PTGS2*) increased to the same levels in both groups following cytokine stimulation, and no differences were observed. MSCs from clinical-grade and Gal-KO pigs were not greatly different from MSCs from non-clinical-grade and WT pigs, and could be used for cell therapy with reduced risk of infection and xenobiotic reaction.

This study demonstrated a method to suppress cell aggregation during the storage of human MSCs, which is important for intravascular administration. In addition, MSCs were established from cryopreserved islets of clinical-grade pigs and bone marrow of Gal-KO pigs, demonstrating that pigs can be used as a source of MSCs. The results of this study are thus useful for further development of MSC-based therapies.

2. General introduction

Stem cell is a general term for cells that have the ability to differentiate into other cells and are capable of proliferating without differentiation. Stem cells can be classified into pluripotent stem cells and somatic stem cells. Pluripotent stem cells are cells that have the ability to differentiate into any cell in the body. Embryonic stem cells (ESCs), which are created from blastocysts, and induced pluripotent stem cells (iPSCs), which are created by artificial gene transfer, are well-known examples [Yamanaka. 2020]. On the other hand, somatic stem cells are cells that exist inside the body and can differentiate into a limited number of cells. Somatic stem cells are slightly more differentiated than pluripotent stem cells. There are many types of somatic stem cells, including hematopoietic stem cells that can differentiate into red blood cells, white blood cells, and platelets [Laurenti *et al*. 2018], neural stem cells that can differentiate into neurons and glial cells [Grochowski *et al*. 2018], and MSCs that can differentiate into bone, cartilage, and fat. In particular, MSCs are one of the stem cells that have attracted specific attention in many clinical studies because of their properties, which will be discussed later.

MSCs are present in a variety of tissues within the body. It has been reported that they can be established from several tissues, including bone marrow [Fu *et al.* 2019], fat [Cai *et al*. 2020], umbilical cord [Keshtkar *et al*. 2020], dental pulp [Gronthos *et al*. 2000], and islets [Davani *et al*. 2007]. In addition, MSCs have shown the potential to differentiate into not only into mesoderm-derived cells such as osteoblasts, chondrocytes, and adipocytes, but also into ectoderm-derived cells such as neurons [Dave *et al*. 2018], endoderm-derived cells such as hepatocytes [Wu *et al*. 2012], and many other cell types. Furthermore, MSCs are known to have the ability to secrete

various cytokines that regulate biological functions. As an example, MSCs can secrete interleukin-10 and transforming growth factor-β [Oh *et al*. 2008], which have anti-inflammatory effects, and prostaglandin E2 [Aggarwal *et al*. 2005], which suppresses immune cells such as natural killer cells, macrophages, and dendritic cells. They also secrete vascular endothelial growth factor [Kagiwada *et al*. 2008], which has angiogenic effects. MSCs themselves have also been shown to have the characteristic of migrating and accumulating at sites of tissue injury and inflammation [Fu *et al*. 2019], and they are thought to be responsible for tissue repair in association with the aforementioned differentiation potential and secreted products. Since MSCs are a heterogeneous cell population, their characteristics, including differentiation potential, secreted cytokines, and migration ability, differ depending on the tissue of origin [Ruetze *et al*. 2014, Cooper *et al*. 2020, Pomatto *et al*. 2021] and culture method [Rombouts *et al*. 2003]. In recent years, the bioactivity and therapeutic effects of exosomes, which are extracellular vesicles secreted by MSCs, have also been actively investigated [Zou *et al*. 2023]. As described above, MSCs are a cell population that exists in many parts of the body and has a wide variety of functions. The minimum criteria of MSCs are: 1. ability to adhere to plastic plates; 2. positive for surface antigens CD105, CD73, and CD90 and negative for CD45, CD34, CD14 or CD11b, CD79a or CD19, and HLA-DR; and 3. ability to differentiate into osteoblasts, chondrocytes, and adipocytes in vitro [Dominici *et al*. 2006].

Regenerative therapy is a medical treatment that aims to restore lost function, e.g., of differentiated cells. Stem cells with the ability to differentiate and repair tissues have been investigated in many studies as a material for regenerative therapy. iPS and ES cells have been used in clinical trials for various diseases such as Parkinson's disease, retinitis pigmentosa, and spinal cord injury [Golchin *et al*. 2021, Tsujimoto *et al*. 2022].

Furthermore, there have been many clinical studies on MSCs [Adas *et al*. 2021, Murata *et al*. 2021, Riordan *et al*. 2018, Dilogo *et al*. 2021], and they have been commercialized as treatments for wounds [Gibbons. 2015], graft-versus-host disease [Konishi *et al*. 2016], and Crohn's disease [Scott. 2018]. In particular, the demand for MSCs as a source of therapeutic cells is expected to continue to increase, since, in contrast to ESCs, the ethical issues associated with the destruction of embryos are avoided, and there is no risk of cancer associated with gene transfer, as is the case with iPSCs.

MSCs are often administered with the expectation of cell and matrix regeneration at sites of injury or concomitant immunosuppressive effects. Several routes of MSC administration have been reported, including via muscle [Berry *et al*. 2019], joints [Yokota *et al*. 2019], and medullary cavity [Staff *et al*. 2019]; however, intravascular administration is the most common [Moll *et al*. 2019]. Further, it has been reported that most MSCs administered via veins accumulate in the pulmonary region, where blood vessels are thin [Rombouts *et al*. 2003]. It is believed that the risk of vascular embolization increases when a large number of cells are rapidly administered into a blood vessel as part of cell therapy. Severe cell embolization in the lungs can be fatal [Tamura *et al*. 1993]. In order to avoid embolization caused by the rapid administration of high concentrations of cells, slow intravascular administration of cells over a period of ~1 hour is the typical approach [Adas *et al*. 2021]. In fact, the guidelines for the use of TEMCELL, a commercial intravenous MSC product in Japan, state the following. 1. Cell administration should be slow to prevent pulmonary embolization. 2. Do not sediment cells by periodically rubbing the infusion bag. 3. Monitor the respiratory status and arterial blood oxygen saturation of the patient receiving the dose.

Generally, cells or tissues that need to be preserved are kept at a low temperature. This is because low temperatures suppress cell and tissue metabolism and prevent

damage due to ATP depletion. However, cells administered to patients via infusion bags or syringes are maintained at room temperature. As mentioned above, cell administration requires a long time, since the cells must be administered slowly in order to prevent embolization. Under such conditions, cell storage and administration solutions must maintain the viability of cells not only at low temperatures but also at room temperature. For intravascular transplantation, cells are often suspended in electrolyte solutions, such as normal saline or saline containing albumin or dextrose [Riordan *et al*. 2018, Murata *et al*. 2021, Dilogo *et al.* 2021, Adas *et al*. 2021]. However, these solutions are not necessarily ideal for maintaining cell viability and preventing cell sedimentation during storage and infusion. Therefore, we developed a better cell preservation solution, “Cellstor”, in which cells can be suspended and stored under refrigeration or at room temperature until use [Fujita *et al*. 2020]. Cellstor was developed by Otsuka Pharmaceutical Factory, Inc. as a cell preservation solution. It is based on lactated Ringer's solution, which has a buffering effect, and contains trehalose, which has a cytoprotective effect. Cellstor S: lactated Ringer’s solution with 3% trehalose and 5% dextran 40 (LR-3T-5D) contains dextran to maintain the suspension and prevent cell sedimentation (Table 1). Cellstor W: lactated Ringer’s solution with 3% trehalose (LR-3T) is a dextran-free product developed for situations where centrifugation is required after cell preservation.

Table 1. Compositions of solutions

Components	LR	LR-3T	LR-3T-5D
Na^+	130 mEq/L	130 mEq/L	130 mEq/L
K^+	4 mEq/L	4 mEq/L	4 mEq/L
Ca^{2+}	3 mEq/L	3 mEq/L	3 mEq/L
Cl^-	109 mEq/L	109 mEq/L	109 mEq/L
$Lactate^-$	28 mEq/L	28 mEq/L	28 mEq/L
Trehalose	-	3%	3%
Dextran-40	-	-	5%

LR: Lactated Ringer's solution.
LR-3T (Cellstor W): Lactated Ringer's solution with 3% trehalose.
LR-3T-5D (Cellstor S): Lactated Ringer's solution with 3% trehalose and 5% dextran 40.

In the storage of human MSCs using LR-3T-5D and LR-3T, cell viability could be maintained for at least 24 h not only at 5 °C but also at 25 °C [Fujita *et al.* 2020]. It is also possible to freeze and thaw human MSCs by adding cryoprotectants such as dimethyl sulfoxide or propylene glycol [Fujita *et al*. 2021]. Furthermore, in addition to human MSCs, it can also be used for short-term preservation of porcine zygotes and porcine blastocysts [Lin *et al*. 2022a, Lin *et al*. 2022b]. LR-3T-5D is a simple and safe component that has potential as a cell administration solution for use in humans. Assuming clinical use, cells suspended in LR-3T-5D were filled into an intravenous infusion bag, and a constant volume of cells could always be dispensed, as cell sedimentation did not occur in the bag even at a slow drip rate [Fujita *et al*. 2020]. Treatment using an infusion bag containing sedimented cells may result in a large amount of cells being administered in a short period of time, posing a risk of embolization if they enter the blood vessels. LR-3T-5D, which suppresses cell sedimentation, can contribute to improving the safety of cell therapy.

On the other hand, it is important that no aggregates are present in the injection material prior to cell administration, as aggregates are also a risk for vascular

embolization [Yaykasli *et al*. 2021]. LR-3T-5D can contribute to the efficacy and safety of cell therapy by maintaining cell viability and suppressing cell sedimentation, but data regarding aggregate development during cell storage is lacking. Therefore, determining the conditions under which cells aggregate and identifying those that suppress aggregation during the preservation stage prior to cell administration would greatly enhance the safety of cell-based therapies.

In order to expand MSC therapy to a wider population, it is very important to establish a stable cell source in addition to ensuring safety. However, several studies have reported difficulties in securing sufficient allogeneic donors to establish a cell bank [Lechanteur *et al*. 2016]. Although it is possible to collect cells from patients themselves, there are safety issues associated with the collection of peripheral blood, bone marrow [Fujimoto *et al.* 2020], and adipose tissue from patients [Kaoutzanis *et al*. 2017]. Moreover, it has been reported that there are differences in the proliferative and differentiation potential and other properties of MSCs depending on the age of the human donor [Liu *et al*. 2020]. There are many challenges in obtaining a large number of sources of allogeneic MSCs with stable properties. We therefore focused on pigs as a potential source of MSCs, as pigs are physiologically and anatomically similar to humans. In addition, since pigs are currently raised on an industrial scale, the technology for stable large-scale production is well established and has the advantage of fewer ethical barriers. Because of their physiological similarities, transplantation of organs from pigs to humans has been performed in recent years [Griffith *et al*. 2022, Montgomery *et al*. 2022], demonstrating that pigs may be useful not only as an organ source but also as a source for cells used as therapeutics.

However, there are two major challenges in using pigs as a source of MSCs as well as for organ transplants. The first is to reduce the risk of infectious diseases

common to pigs and humans. There are several known infectious diseases common to pigs and humans, including toxoplasmosis and hepatitis E. There is a risk of humans contracting these infections when pig tissues and cells are used for transplantation [Fishman. 2018], an issue that must be resolved for pigs to be used as a source of MSCs. Therefore, we focused on clinical-grade pigs with controlled infection risk as a source of MSCs for clinical applications. Clinical-grade pigs are pathogen-free pigs that have been created, assessed, and maintained in an isolated barrier facility, as mentioned in the discussion of xenotransplantation regulations [Schuurman. 2015]. Previously, we isolated and cultured mesenchymal stem cells from clinical-grade neonatal porcine bone marrow (npBM-MSCs) and characterized them [Nishimura *et al*. 2019]. Furthermore, we confirmed the therapeutic efficacy of porcine-derived MSCs by transplanting npBM-MSCs into mouse models of ischemic limb disease and diabetic wound healing [Yamada *et al*. 2021, Yamada *et al*. 2022]. The therapeutic application of these cells is a subject of ongoing investigation.

It is extremely useful to have a stable supply of cells or cell source tissues that can be cryopreserved to ensure a consistent supply of cells for therapeutic use. In addition, MSCs can be established from a variety of tissues, but their proliferative and secretory characteristics are known to vary depending on the tissue of origin [Ruetze *et al*. 2014]. In order to maximize the therapeutic efficacy of MSCs, it is necessary to characterize MSCs by origin. Therefore, in this study, we investigated the establishment and characteristics of MSCs using cryopreserved islets from clinical-grade pigs.

The second issue in using pigs as a source of MSCs is the need to suppress xenogeneic rejection between humans and pigs. Even in human-to-human transplants, the transplanted organs and cells are recognized by the immunological system as non-self and rejected. There are various types of rejection. The major problem in human-to-

human transplantation is acute rejection, in which the recipient's T cells recognize non-self cell surface antigens such as human leukocyte antigen HLA. These are expressed by almost all transplanted cells, and initiate an attack on the transplanted cells. Acute rejection is a cell-based reaction that often occurs within days to weeks after transplantation. Many drugs that suppress T cells, such as cyclosporine and tacrolimus, can reduce acute rejection. On the other hand, when porcine tissue is transplanted into humans, the transplanted organ is abolished within a few minutes to a few hours after transplantation; this is known as "hyperacute rejection". In this reaction, the natural antibodies present in human blood react with pig cell surface antigens such as galactosyl-alpha 1,3-galactose antigen (Gal), which activates complement and causes blood clots and cell damage. Hyperacute rejection is mediated by complement in the blood; thus, immunosuppressive drugs that suppress the cellular response are less effective. It has been reported that prior removal of antibodies from the recipient's blood by plasma exchange can reduce the occurrence of hyperacute rejection, but long-term survival is challenging [Makowka *et al*. 1994].

In recent years, in order to suppress hyperacute rejection in xenotransplantation, studies of antigen removal on porcine cells using, e.g., genome editing technology have been conducted. This approach is effective in suppressing hyperacute rejection [Griffith *et al*. 2022, Montgomery *et al*. 2022]. We have also used genome editing technology to produce pigs with suppressed porcine cell surface antigens, such as Gal, glycans modified with N-glycolylneuraminic acid, and Sda, in order to control hyperacute rejection [Tanihara *et al*. 2020, Tanihara *et al.* 2022]. Therefore, we studied whether MSCs from Gal-KO pigs could be used as a source of cell therapy by attempting to establish MSCs from Gal-KO pigs and characterizing them in comparison with wild type pigs.

3. Avoiding aggregation of human bone marrow–derived mesenchymal stem cells stored in cell preservation solutions

3.1 Introduction

Mesenchymal stem cells (MSCs) are widely used in clinical practice, most commonly administered intravascularly [Moll *et al.* 2019]. Rapid, high-dose administration of cells into blood vessels increases the risk of vascular embolization; thus, intravascular cells are administered slowly over a period of approximately 1 h [Adas *et al.* 2021]. Cells are typically administered at room temperature, and the cells are often suspended in a saline solution with or without dextrose [Riordan *et al.* 2018, Adas *et al.* 2021, Dilogo *et al.* 2021, Murata *et al.* 2021]. We considered that saline solution is not an ideal medium for cell administration performed slowly at room temperature; therefore, we developed several improved cell preservation solutions, namely, lactated Ringer's solution containing 3% trehalose (LR-3T) and lactated Ringer's solution containing 3% trehalose and 5% dextran 40 (LR-3T-5D). LR-3T maintains cell viability during storage for up to 24 h under refrigeration or at room temperature. The risk of vascular embolization is thought to increase during rapid cell administration. As sedimentation of cells in the infusion line can increase the rate of cell administration, it is necessary to equalize the cell concentration throughout the suspension. Dextran, a component of LR-3T-5D, suppresses cell sedimentation and thereby helps maintain a stable concentration of cells in the infusion line [Fujita *et al.* 2020]. This solution was shown to improve the preservation of porcine embryos [Lin *et al.* 2022a, Lin *et al.* 2022b], and the addition of dimethyl sulfoxide or propylene glycol allows solutions to be used for cryopreservation [Fujita *et al.* 2021] of, for example, porcine bone marrow–derived MSCs [Nishimura *et*

al. 2019, Kikuchi *et al.* 2021].

Aggregates in blood vessels can cause embolization in microvessels [Yaykasli *et al.* 2021]; thus, cells administered into blood vessels must be non-aggregated. The risk of embolization is particularly high in the lungs due to the high number of microvessels. The efficacy of intravascular administration of MSCs for treating coronavirus infectious disease–2019 (COVID-19)–related acute respiratory distress syndrome was recently reported [Qu *et al.* 2022], heightening the importance of obtaining safety information on the aggregation of administered cells.

In this study, we investigated the conditions under which cell aggregation occurs and methods for suppressing this aggregation by varying preservation time, temperature, and trypsin treatment time using human bone marrow–derived (hBM)-MSCs stored in LR-3T and LR-3T-5D.

3.2 Materials and methods

3.2.1 Preservation solutions

Lactated Ringer's solution (LR; Lactec® Injection), LR-3T (Cellstor-W), and LR-3T-5D (Cellstor-S) were supplied by Otsuka Pharmaceutical Factory, Inc. (Tokushima, Japan). LR-3T and LR-3T-5D were developed as cell preservation solutions. Both of these solutions maintain the viability and function of hADSCs for at least 24 h under refrigeration or at room temperature, and LR-3T-5D is designed to keep cells suspended during infusion [Fujita *et al.* 2020].

3.2.2 Preparation of hBM-MSCs

hBM-MSCs (male, 31Y, lot no. 0000527428; Lonza Walkersville, Inc. Walkersville, MD, USA) were used in this study, where 31Y indicates the age in years of the donor. The hBM-MSCs were seeded in a 75 cm^2 flask with 15 mL of medium prepared from a medium kit (PT-3001 MSCGM™ BulletKit™, Lonza Walkersville, Inc.) and maintained at 37°C in a humidified 5% CO_2 atmosphere. The medium was changed every 3 or 4 days; the cells were passaged at approximately 80% confluency, and passages 4 or 5 (5 or 6 after cell preparation) were used for experiments. Cells were washed with phosphate-buffered saline without calcium and magnesium (PBS[−]) and trypsinized using trypsin/EDTA solution (CC-3232, Lonza Walkersville, Inc.) at 25 °C for 3.5-4 min or for a predetermined time. The trypsin reaction was stopped by addition of culture medium, and the hBM-MSCs were subsequently detached by pipetting. The supernatant containing hBM-MSCs was transferred to a 50 mL conical tube and centrifuged at 600 × *g* for 5 min at room temperature. After the supernatant was aspirated, hBM-MSCs (5×10^5 cells/mL) were resuspended in LR or PBS(−) for use in storage experiments.

3.2.3 Cell aggregation

After storage, the cells were suspended thoroughly and gradually. The total numbers of cells and cell aggregates were determined using a NucleoCounter® NC-200™ (ChemoMetec A/S, Allerød, Denmark). Cell aggregation was defined as an association of ≥5 cells (Figure 3.1). The cell aggregation rate (%) was calculated from the total number of cells counted.

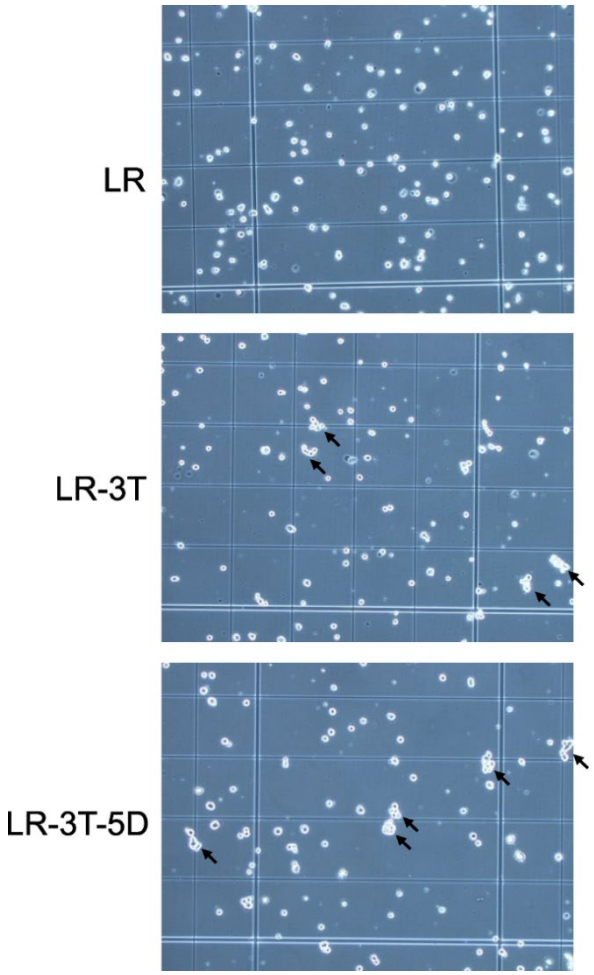

Figure 3.1. Micrographs of human bone marrow–derived stem cells (hBM-MSCs) after storage at 25 °C for 24 h in lactated Ringer's solution (LR), LR with 3% trehalose (LR-3T), or LR-3T with 5% dextran 40 (LR-3T-5D) (magnification 100×). Arrows indicate cell aggregates.

3.2.4 Cell viability

After storage, the cells were stained with trypan blue to assess viability. The total number of cells and number of dead cells were determined manually using a plastic cell-counting plate (OneCell Counter, Bio Medical Science, Ltd. Tokyo, Japan). Cell aggregates were excluded from the cell counts. Cell viability was calculated according to the following formula:

Cell viability [%] = (total number of cells − number of dead cells)/(total number of cells) × 100.

3.2.5 Experimental design

The present study was approved by the Ethics Committee of Otsuka Pharmaceutical Factory, Inc. The first experiment examined the effect of storage time on the aggregation and viability of hBM-MSCs stored in LR, LR-3T, or LR-3T-5D at 25 °C. After centrifugation at 600 × *g* for 5 min, the cells were resuspended at a density of 5 × 10^5 cells/mL in LR, LR-3T, or LR-3T-5D, and 500 μL aliquots of each cell suspension were transferred to low–cell adsorption 15 mL tubes (STEMFULL™, Sumitomo Bakelite Co. Ltd. Tokyo, Japan). The tubes were tightly capped and then stored at 25 °C in an incubator for various times (0, 1, 3, 6, and 24 h).

The second experiment examined the effect of storage temperature on aggregation and viability of hBM-MSCs stored at 5 or 25 °C for 24 h in LR-3T-5D, the solution in which the greatest amount of cell aggregation occurred in the first experiment. As described above, the cells were resuspended in LR-3T-5D at a density of

5×10^5 cells/mL, and 500-µL aliquots of the cell suspension were transferred to separate tubes and stored for 24 h at 25 °C and 5 °C.

The third experiment examined the effect of trypsinization treatment time during cell collection on aggregation and viability of hBM-MSCs stored at 25 °C for 24 h in LR-3T-5D. Immediately following cell collection from the flasks, the cells were trypsinized with trypsin/EDTA solution for 5 or 10 min at 25 °C and resuspended in LR-3T-5D at a density of 5×10^5 cells/mL. The cell suspensions (500 µL each) were transferred to separate tubes and stored for 24 h at 25 °C.

3.2.6 Data analysis and statistics

Data are presented as the mean ± standard deviation (SD). Statistical analysis was performed using two-tailed tests (Dunnett's multiple comparison test, Tukey's test, or non-paired Student's *t*-test). Data were analyzed using SAS 9.4 software (SAS Institute, Inc. Cary, NC, USA).

3.3 Results

3.3.1 Effect of storage time on the aggregation and viability of hBM-MSCs stored in LR, LR-3T, or LR-3T-5D at 25 ℃

As shown in Figure 3.2A, there were no significant differences in cell aggregation rates after storage in each solution at 25 °C for up to 6 h compared with before storage (Pre). However, the aggregation rate of hBM-MSCs stored in LR-3T or LR-3T-5D for 24 h was significantly higher ($p<0.01$) than the pre-storage rate. A comparison between

solutions at each time point showed that storage in LR-3T-5D resulted in significantly higher aggregation than storage in LR-3T or LR at 6 h ($p<0.01$) and higher than LR at 24 h ($p<0.05$).

When stored at 25 °C for 24 h, the viability of hBM-MSCs stored in LR was significantly lower ($p<0.001$) than the pre-storage rate, whereas the viability of cells stored in LR-3T or LR-3T-5D was comparable to the pre-storage rate (Figure 3.2B). In addition, the viability of hBM-MSCs stored in LR was significantly lower than that of cells stored in LR-3T-5D for 1, 3, or 24 h ($p<0.05$) and lower than that of cells stored in LR-3T for 24 h ($p<0.05$).

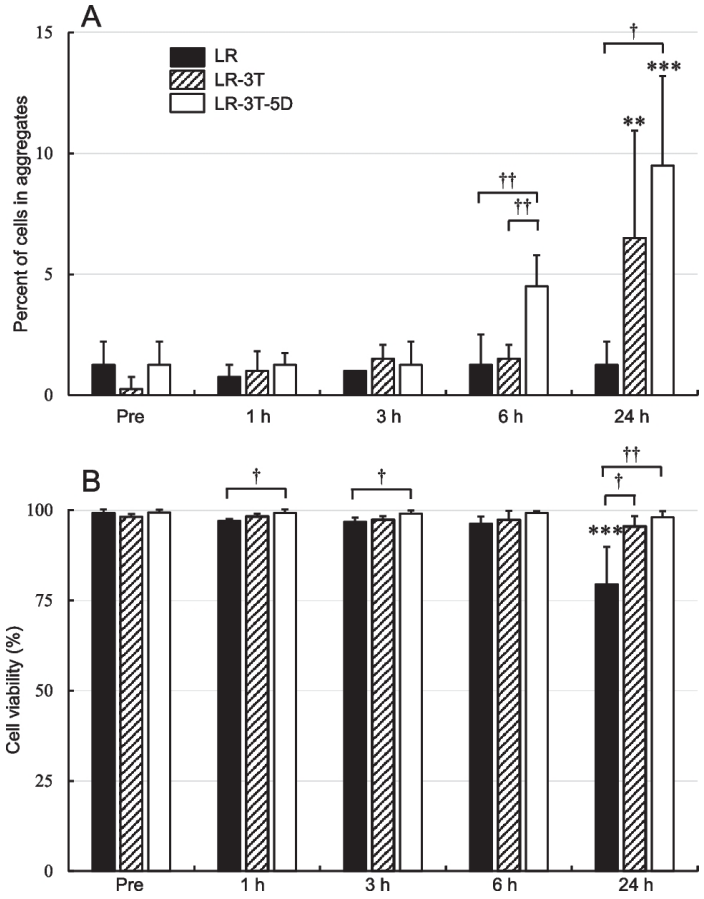

Figure 3.2. Aggregation rate (A) and viability (B) of hBM-MSCs after storage at 25°C for various times in LR, LR-3T, or LR-3T-5D. Data are presented as the mean ± SD (n = 4). Statistical analysis was performed using two-tailed Dunnett's test vs. before storage (Pre): **p<0.01, ***p<0.001, and using two-tailed Tukey's test: †p<0.05, ††p<0.01.

3.3.2 Effect of storage temperature on the aggregation and viability of hBM-MSCs stored in LR-3T-5D

As shown in Figure 3.3A, the aggregation rate of hBM-MSCs stored in LR-3T-5D for 24 h at 25 °C was significantly higher ($p<0.01$) than the pre-storage rate, whereas the aggregation rate of hBM-MSCs stored in LR-3T-5D for 24 h at 5 °C was similar to the pre-storage rate. The viability of hBM-MSCs stored in LR-3T-5D for 24 h at 5 °C and 25 °C was similar to the pre-storage viability (Figure 3.3B)

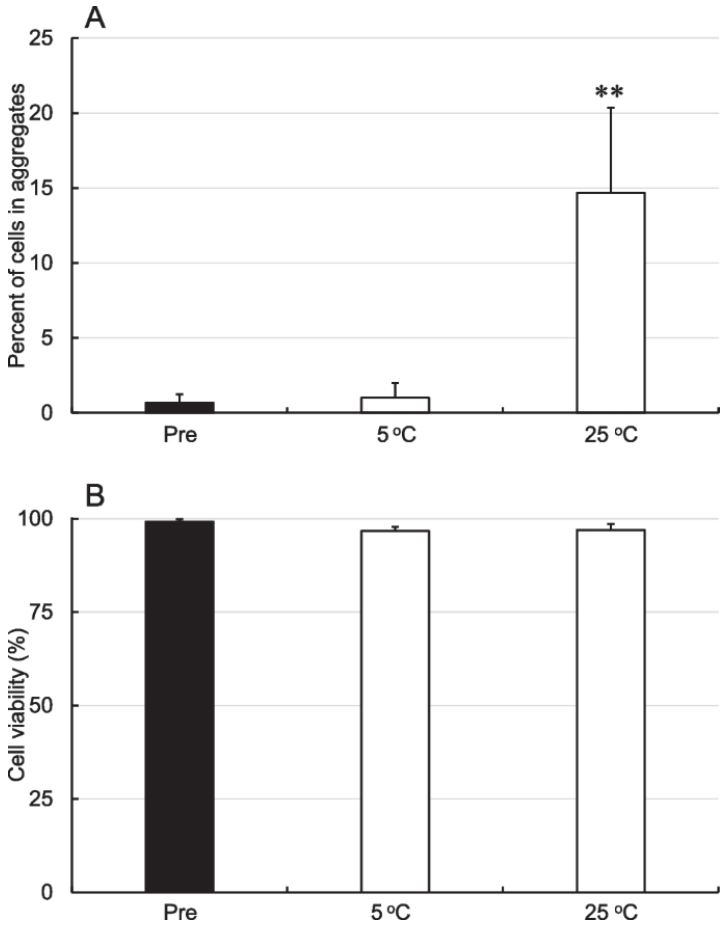

Figure 3.3. Aggregation rate (*A*) and viability (*B*) of hBM-MSCs after storage at 5 or 25°C for 24 h in LR-3T-5D. Data are presented as the mean ± SD (n = 3). Statistical analysis was performed using two-tailed Dunnett's test vs. before storage (Pre): **p<0.01.

3.3.3 Effect of trypsinization time before storage on the aggregation and viability of hBM-MSCs

As shown in Figure 3.4A, when, the aggregation rate after storage of hBM-MSCs trypsinized for 10 min for cell collection was significantly lower than that of cells trypsinization for 5 min ($p<0.05$). There was no significant difference in cell viability, however (Figure 3.4B).

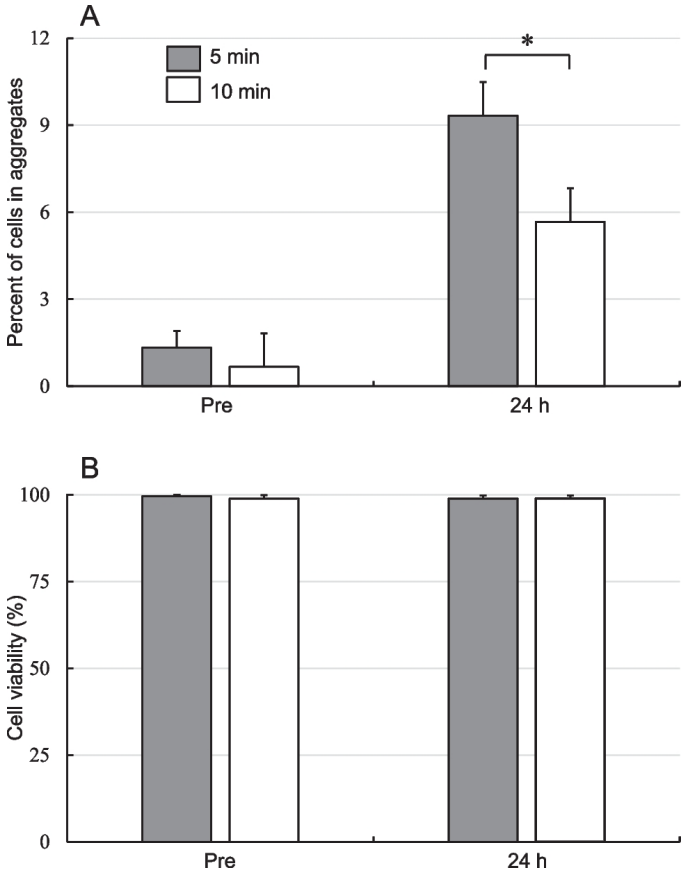

Figure 3.4. Aggregation rate (A) and viability (B) of hBM-MSCs collected by trypsinization for 5 or 10 min and stored in LR-3T-5D for 24 h at 25°C. Data are presented as the mean ± SD (n = 3). Statistical analysis was performed using two-tailed non-paired t-test: *$p<0.05$.

3.4 Discussion

MSCs are adhesive cells, and one of their characteristics is that they adhere to containers during culture [Dominici *et al.* 2006]. The use of low-adhesion test tubes (STEMFULL™) avoids adherence to containers and improves the cell recovery ratio after storage. On the other hand, MSCs also adhere to each other and form spheroids when cultured in low-adhesion containers [Cesarz *et al.* 2016]. Therefore, in this study, we confirmed that hBM-MSCs aggregate upon storage at 25 °C for 24 h in LR-3T-5D or LR-3T.

When stored in LR at 25°C, no cell aggregates were observed, even after 24 h, but cell viability was decreased compared with cells stored in LR-3T-5D or LR-3T and with cells before storage in LR. It has been suggested that cells with low viability show low adhesion and proliferation in colony-forming assays [Fujita *et al.* 2021]. Our observations may also indicate that a decline in cell viability during storage would be associated with low cell aggregation.

Storage in LR-3T-5D at 25 °C for 6 h resulted in more cell aggregation than when cells were stored in LR-3T. The difference between the two solutions is the presence or absence of dextran 40. The dextran 40 in LR-3T-5D inhibits the sedimentation of cells in bags or syringes and helps maintain a given concentration of cells at the time of administration [Fujita *et al.* 2020]. However, dextran coatings reportedly enhance the adhesion of BM-MSCs to sponge scaffolds [Togami *et al.* 2014]; thus, the adhesion-enhancing effect of dextran 40 may be responsible for the observed high degree of cell aggregation in LR-3T-5D at room temperature. In contrast, at 5 °C, no agglomerates formed, even after 24 h of storage in LR-3T-5D. The expression of membrane proteins such as cadherins may play an important role in MSC adhesion [Wuchter *et al.* 2007].

The mechanism of storage-associated cell aggregation remains unclear, but cell aggregation may be inhibited due to the suppression of membrane protein function at low temperatures.

The aggregation of cells stored in LR-3T-5D at 25 °C for 24 h was suppressed by a trypsin treatment time of 10 min instead of 5 min for cell collection before storage. There was no change in cell viability after 10 min of trypsin treatment; thus, cell aggregation was not inhibited due to a decrease in viability, as was the case when cells were stored at 25 °C for 24 h in LR. A number of reports have indicated that trypsin treatment decreases the expression of surface proteins on MSCs [Tsuji *et al.* 2017, Garg *et al.* 2014, Nakao *et al.* 2019]. High concentrations of trypsin were shown to suppress CXCR4 expression in BM-MSCs [Pervin *et al.* 2021]. N-cadherin is required for the aggregation of HEK293T cells after trypsin detachment, and suppressing N-cadherin also suppresses aggregation [Tachibana. 2019]. We therefore believe that a trypsin treatment time of 10 min suppresses the function of surface proteins involved in adhesion, including cadherins, thereby also suppressing storage-associated aggregation.

3.5 Conclusions

This study showed that storage of hBM-MSCs in LR-3T or LR-3T-5D for 24 h at 25 °C is associated with high cell aggregation rates, although cell viability is maintained. In contrast, aggregation is suppressed when the cells are stored at 5 °C. Furthermore, cell aggregation might be suppressed by prolonging the length of trypsinization from 5 min to 10 min.

4. Relationship between oxygen partial pressure and inhibition of cell aggregation of human adipose tissue-derived mesenchymal stem cells stored in cell preservation solutions

4.1 Introduction

Stem cell transplantation is a promising therapy for various diseases, such as Coronavirus Infectious Disease–2019 (COVID-19)–related Acute Respiratory Distress Syndrome [Qu *et al.* 2022], cardiovascular disorders [Terashvili *et al.* 2019], autoimmune diseases [Munir *et al.* 2015], osteoarthritis [Wyles *et al.* 2015], liver disorders [Kholodenko *et al.* 2017], and graft-versus-host disease [Trounson *et al.* 2015]. Among stem cells, mesenchymal stem cells (MSCs) are attractive because of their multi-potency in differentiation, immunosuppressive effects, and remodeling effects on extracellular matrices. For intravascular transplantation, cells are often suspended in electrolyte solutions, such as normal saline or saline containing albumin or dextrose [Murata at al. 2021, Riordan *et al.* 2018, Dilogo *et al.* 2021, Adas *et al.* 2021]. However, these solutions are not necessarily ideal for maintaining cell viability and preventing the sedimentation of cells during storage and infusion. Therefore, we developed a better cell preservation solution in which cells can be suspended and stored under refrigeration or at room temperature until use [Fujita *et al.* 2020]. This solution can also preserve porcine zygotes [Lin *et al.* 2022a]. The addition of curcumin to this solution was shown to improve the preservation of porcine embryos [Lin *et al.* 2022b], and the addition of dimethyl sulfoxide or propylene glycol allows solutions to be used for cryopreservation [Nishimura *et al.* 2019] of, for example, porcine bone marrow–derived MSCs [Kikuchi *et al.* 2021].

Severe cell embolization in the lungs can be fatal [Tamura *et al.* 1993]. It is believed that the risk of vascular embolization increases when a large number of cells are rapidly administered into a blood vessel as part of cell therapy; therefore, preventative measures are generally taken during the procedures, such as administering cells slowly [Adas *et al.* 2021]. Indeed, some intravenously administered cell preparations currently on the market prescribe a slow rate of cell administration. In addition to the effect of administration rate, the risk of embolization is elevated when administering populations of large cells, such as pancreatic islets [Yin *et al.* 2006]. Because adherent cells naturally exhibit a potential to adhere to each other and form large cell populations, cell aggregation should be considered when administering adherent cells via blood vessels.

Generally, cells or tissues that need to be preserved are kept at a low temperature. However, when cells are administered to patients via infusion bags or syringes, they are maintained at room temperature. As mentioned above, cell administration requires a long time because the cells are administered slowly in order to prevent embolization. Under such conditions, cell storage and administration solutions must maintain the viability of the cells not only at low temperatures but also at room temperature [Fujita *et al.* 2020].

To date, there have been no reported studies examining the occurrence and inhibition of MSC aggregation under room temperature storage and administration conditions. Therefore, we examined the storage conditions under which aggregation occurs and the conditions that inhibit aggregation when human adipose tissue-derived mesenchymal stem cells (hADSCs) are stored in a solution developed for storage at room temperature.

4.2 Materials and methods

4.2.1 Preservation solutions

Lactated Ringer's solution (LR; Lactec® Injection) and lactated Ringer's solution with 3% trehalose and 5% dextran 40 (LR-3T-5D; Cellstor-S) were supplied by Otsuka Pharmaceutical Factory, Inc. (Tokushima, Japan). The LR-3T-5D was developed as a cell-preservation solution in which cells can be suspended and stored under refrigeration or at room temperature [Fujita *et al.* 2020].

4.2.2 Preparation of adipose tissue-derived mesenchymal stem cells

hADSCs (female, 38Y and 44Y, PT5006, lot nos. 0000421627 and 0000692059, respectively; Lonza Walkersville, Inc., Walkersville, MD, USA) were used in this study; 38Y and 44Y indicate the donors' age in years. The hADSCs were seeded in a 75 cm^2 flask with 15 mL of medium prepared from a medium kit (PT-4505 ADSC BulletKit™, Lonza Walkersville, Inc.) and maintained at 37 °C in a humidified 5% CO_2 atmosphere. The medium was changed every 3 or 4 days; the cells were passaged at approximately 90% confluency, and passages 3, 4, or 5 (4, 5, or 6 after cell preparation) were used for experiments. Cells were washed with phosphate-buffered saline without calcium and magnesium and trypsinized with trypsin/EDTA solution (CC-5012, Lonza Walkersville, Inc.) for 3-5 min at 37 °C. The trypsin reaction was stopped by addition of trypsin-neutralizing solution (CC-5002, Lonza Walkersville, Inc.), and hADSCs were subsequently detached by pipetting. The supernatant

containing hADSCs was transferred to a 50 mL conical tube and centrifuged at 210 × *g* for 5 min at room temperature. The supernatant was aspirated, and hADSCs were resuspended in LR for use in storage experiments.

4.2.3 Cell aggregation

After storage, samples of cells in the tubes were slowly but thoroughly re-suspended. The total numbers of cells and cell aggregates were determined using a NucleoCounter® NC-200™ (ChemoMetec A/S, Allerød, Denmark). Cell aggregation was defined as an association of ≥5 cells (Figure 4.1). This is because it is difficult to measure more than 5 cells in a three-dimensional cell mass. The cell aggregation rate (%) was calculated from the total number of cells counted.

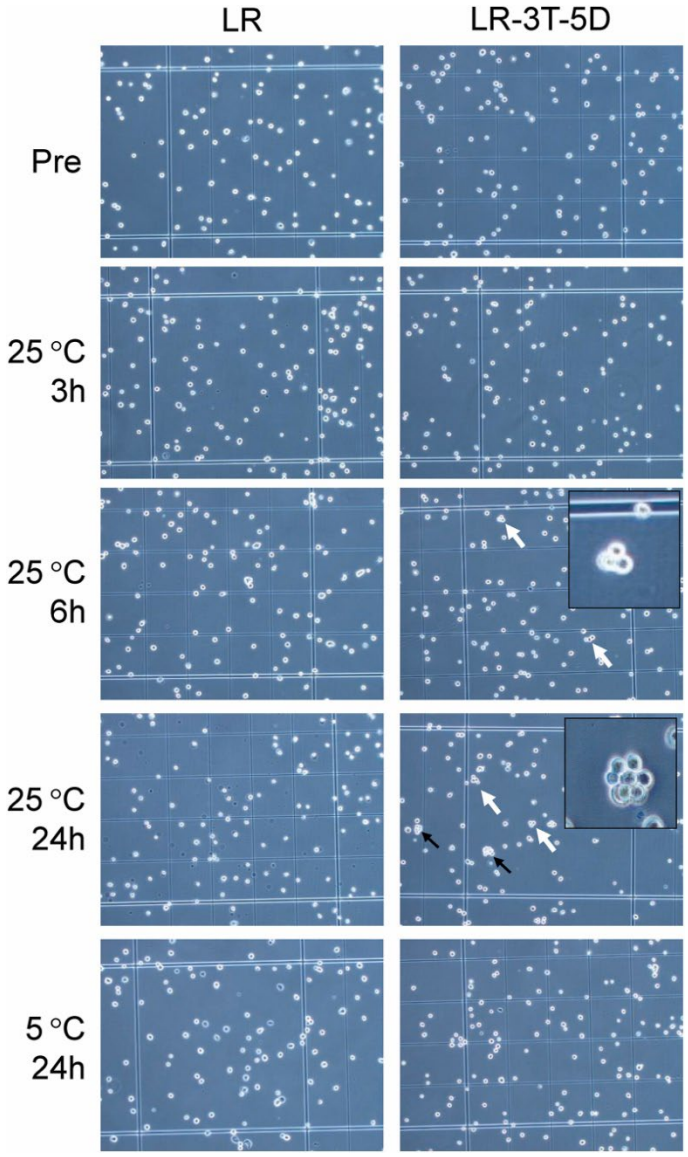

Figure 4.1. Micrographs of human adipose tissue–derived stem cells (hADSCs) after storage at 5 °C 24 h and 25 °C for each hour in lactated Ringer's solution (LR) and LR with 3% trehalose and 5% dextran 40 (LR-3T-5D) (magnification 100×). Black arrows indicate cell aggregates (≥5 cells) and white arrows indicate cell clusters of 4 ≤ cells. Inset shows a magnified image of the aggregated cells and cell clusters of 4 ≤ cells.

4.2.4 Cell viability

After storage, cells were stained with trypan blue to assess viability. The total numbers of cells and dead cells were determined manually using a plastic cell-counting plate

(OneCell Counter, Bio Medical Science, Ltd., Tokyo, Japan). Cell aggregates were excluded from the cell counts. Cell viability was calculated according to the following formula:

Cell viability [%] = (total number of cells − number of dead cells)/(total number of cells) × 100.

4.2.5 Oxygen partial pressure (pO_2) in storage solution

After storage, the cells in each tube were not re-suspended prior to pO_2 measurement, which was carried out immediately after sampling according to a standard method using a RAPIDLab348EX Blood Gas System analyzer (Siemens Healthcare K.K., Japan).

4.2.6 Experimental design

The present study was approved by the Ethics Committee of Otsuka Pharmaceutical Factory, Inc. The first experiment examined the effects of storage temperature and time on the aggregation and viability of hADSCs stored in LR and LR-3T-5D. After centrifugation at 210 × *g* for 5 min, the cells were re-suspended at a density of 5×10^5 cells/mL using either LR or LR-3T-5D, and 500 µL of each cell suspension was transferred to low–cell adsorption tubes (STEMFULL™, Sumitomo Bakelite Co., Ltd., Tokyo, Japan). The tubes (15 mL) were tightly capped and stored at 5 °C in a refrigerator or at 25 °C in an incubator for various times up to 24 h.

The second experiment examined the effect of storage volume on aggregation, pO_2, and viability of hADSCs stored with LR-3T-5D, which was able to maintain viability at 25 °C for 24 h. As described above, the cells were re-suspended in LR-3T-

5D at a density of 5×10^5 cells/mL, and 250, 500, 1,000, and 2,000 μL of cell suspension was transferred to separate tubes and stored for 24 h at 25 °C in an incubator.

The third experiment examined the effect of cell density on the aggregation, pO_2, and viability of hADSCs stored in LR-3T-5D. As described above, the cells were re-suspended in LR-3T-5D at densities of 2×10^6, 1×10^6, 5×10^5, and 2.5×10^5 cells/mL, and 500 μL of cell suspension was transferred to separate tubes and stored for 24 h at 25 °C in an incubator.

The fourth experiment examined the effect of nitrogen gas replacement on the aggregation, pO_2, and viability of hADSCs. As described above, the cells were re-suspended in LR-3T-5D at a density of 5×10^5 cells/mL, and 250 μL of each cell suspension was transferred to separate tubes. The solution volume was selected as that most likely to cause aggregation based on a prior experiment. A sufficient amount of filter-sterilized nitrogen gas was blown into the sample tubes for 5 sec, and then the tubes were tightly capped and stored for 24 h at 25 °C in an incubator. In all experiments, cell samples in tubes were stored under static condition.

4.2.7 Data analysis and statistics

Data are presented as the mean ± standard deviation (SD). Statistical analysis was performed using two-tailed tests, consisting of either a Dunnett's multiple comparison test or a non-paired Student's *t*-test. Data were analyzed using SAS 9.4 software (SAS Institute, Inc., Cary, NC, USA).

4.3 Results

4.3.1 Effects of storage temperature and time on the aggregation and viability of hADSCs stored in LR and LR-3T-5D

As shown in Figure 4.2A, there were no significant differences in the aggregation rates of hADSCs stored in LR at 5 °C and 25 °C for up to 24 h compared with pre-storage rates (Pre). However, the aggregation rate of hADSCs stored in LR-3T-5D at 25 °C for 24 h was significantly higher ($p < 0.001$) than the pre-storage rate. When hADSCs were stored at 25 °C for up to 6 h, the aggregation rate did not differ between cells stored in LR versus LR-3T-5D, but the aggregation rate was significantly higher ($p < 0.05$) for cells stored in LR-3T-5D than that of cells stored in LR at either 25 °C or 5 °C for 24 h.

The viability of hADSCs stored in LR at 5 °C or 25 °C for 24 h was significantly lower ($p < 0.05$) than the pre-storage viability, but the viability of cells stored in LR-3T-5D was comparable to the pre-storage viability (Figure 4.2B). In addition, the viability of hADSCs stored at 25 °C for up to 6 h did not differ between cells stored in LR versus LR-3T-5D, but the viability of cells stored in LR-3T-5D at either 25 °C or 5 °C for 24 h was significantly higher ($p < 0.01$) than that of cells stored in LR.

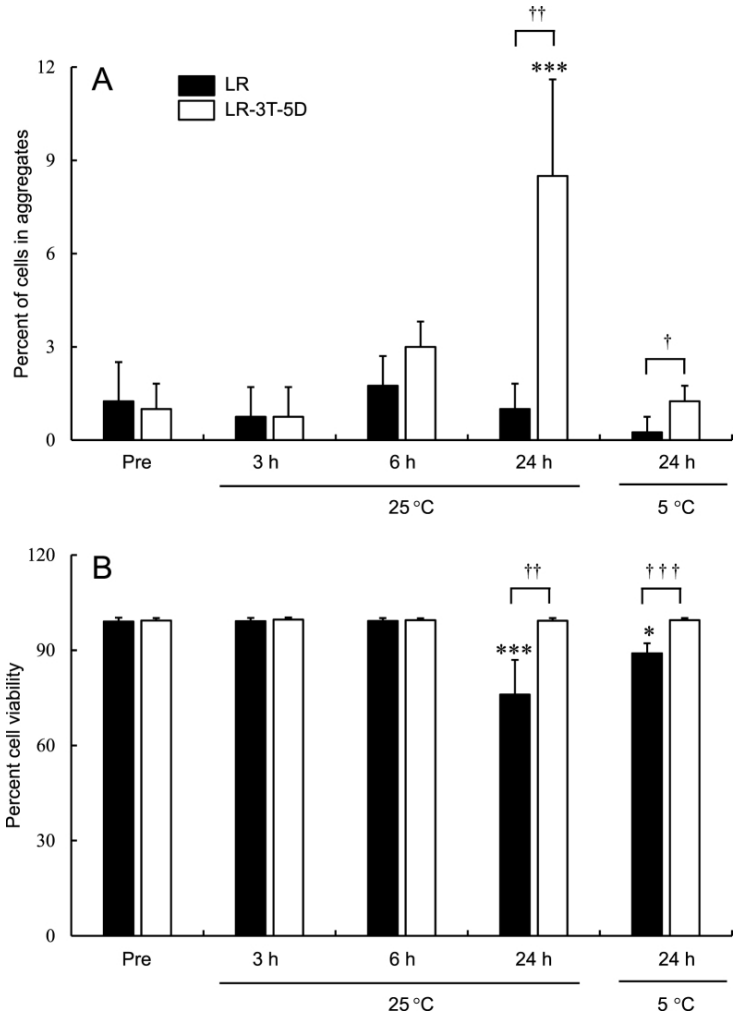

Figure 4.2. Aggregation rate (A) and viability (B) of hADSCs after storage at 5 °C and 25 °C for various times in lactated Ringer's solution (LR) and LR-3T-5D. Data are presented as the mean ± SD (n = 4). Statistical analysis was performed using two-tailed Dunnett's test vs. before storage (Pre): ∗p < 0.05, ∗∗p < 0.001, and using two-tailed non-paired *t*-test: †p < 0.05, ††p < 0.01, †††p < 0.001.

4.3.2 Effect of storage volume on the aggregation, pO_2, and viability of hADSCs

When hADSCs (5×10^5 cells/mL) were stored at 25 °C for 24 h in various volumes (250-2,000 μL) of LR-3T-5D, the aggregation rate tended to decrease with increasing solution volume (Figure 4.3A). The aggregation rates of cells stored in 250, 500, and 1,000 μL of LR-3T-5D were significantly higher ($p < 0.01$) than the pre-storage rates. Moreover, the aggregation rate in 2,000 μL was significantly lower ($p < 0.01$) than that of cells stored in 250 μL of LR-3T-5D. The post-storage pO_2 was significantly lower ($p < 0.01$) than that before storage, irrespective of storage volume (Figure 4.3B). Moreover, the pO_2 tended to decrease with increasing solution volume. The pO_2 was significantly lower ($p < 0.001$) in cell samples stored in 1,000 μL and 2,000 μL of LR-3T-5D than in cell samples stored in 250 μL. There were no significant differences in cell viability among the different storage volumes (Figure 4.3C).

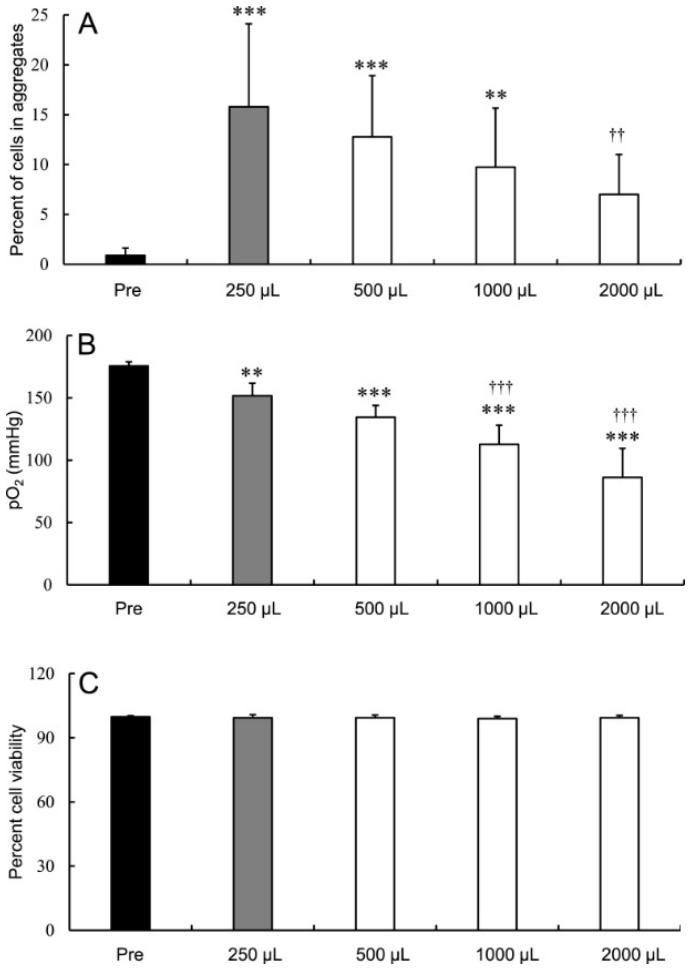

Figure 4.3. Aggregation rate (A), oxygen partial pressure (pO_2) in the preservation solution (B), and viability (C) of hADSCs after storage at 25 °C for 24 h in various volumes of LR-3T-5D. Data are presented as the mean ± SD (n = 8–14). Statistical analysis was performed using two-tailed Dunnett's test vs. before storage (Pre): ∗∗p < 0.01, ∗∗∗p < 0.001, and vs. 250 µL: ††p < 0.01, †††p < 0.001.

4.3.3 Effect of cell density on the aggregation, pO_2, and viability of hADSCs

When hADSCs were stored in LR-3T-5D at 25 °C for 24 h at various densities (2.5-20 × 10^5 cells/mL), the cell aggregation rate tended to decrease with increasing cell density (Figure 4.4A). Compared with the pre-storage rates, the post-storage cell aggregation rates were significantly higher ($p < 0.01$) for samples stored at densities <5 × 10^5 cells/mL. Moreover, the cell aggregation rates decreased at densities >10 × 10^5 cells/mL compared with 2.5 × 10^5 cells/mL. The post-storage pO_2 was significantly lower ($p < 0.001$) than that before storage, irrespective of cell density. Compared with a density of 2.5 × 10^5 cells/mL, the pO_2 was significantly lower ($p < 0.001$) at densities >5 × 10^5 cells/mL (Figure 4.4B). There were no significant differences in viability among cells stored at different densities (Figure 4.4C).

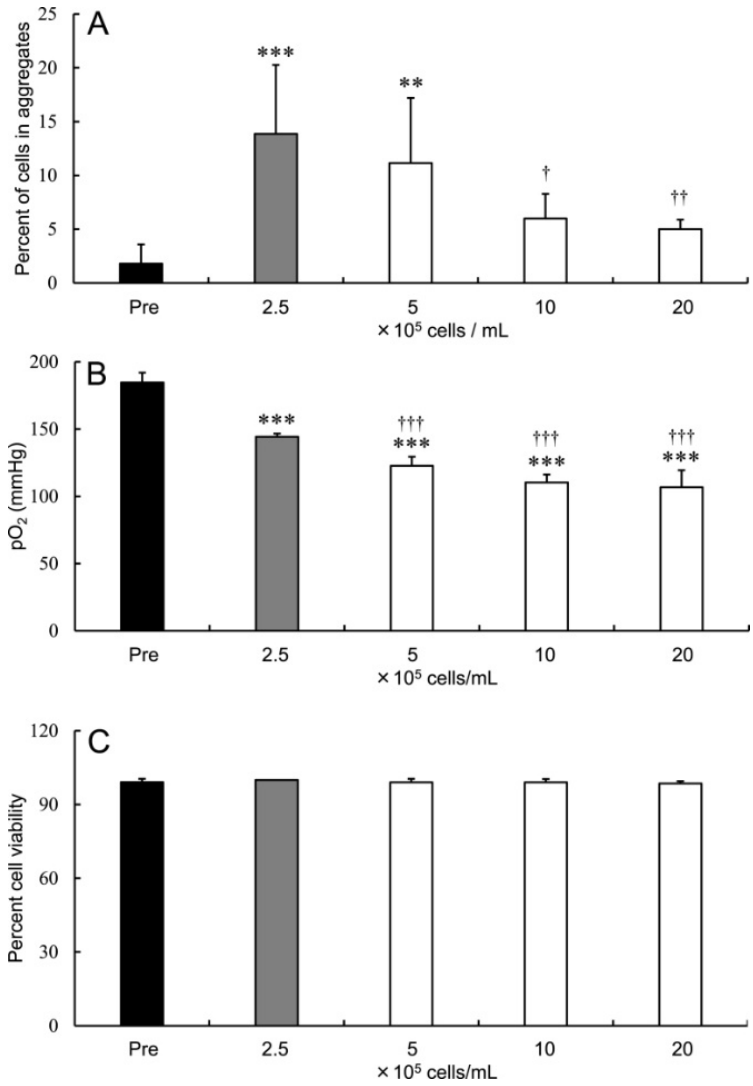

Figure 4.4. Aggregation rate (A), pO_2 in the preservation solution (B), and viability (C) of hADSCs after storage at various cell densities at 25 °C for 24 h in LR-3T-5D. Data are presented as the mean ± SD (n = 5–7). Statistical analysis was performed using two-tailed Dunnett's test before storage (Pre): ∗∗p < 0.01, ∗∗∗p < 0.001, and vs. 2.5 × 10^5 cells/mL: †p < 0.05, ††p < 0.01, †††p < 0.001.

4.3.4 Effect of nitrogen gas replacement on the aggregation, pO_2, and viability of hADSCs

Replacement of the head gas in sample tubes with nitrogen significantly decreased the cell aggregation rate and reduced the pO_2 from a mean of 139.2 mmHg to 46.6 mmHg ($p < 0.05$) (Figure 4.5A and B). However, there was no difference in viability between hADSCs stored with versus without nitrogen gas replacement (Figure 4.5C).

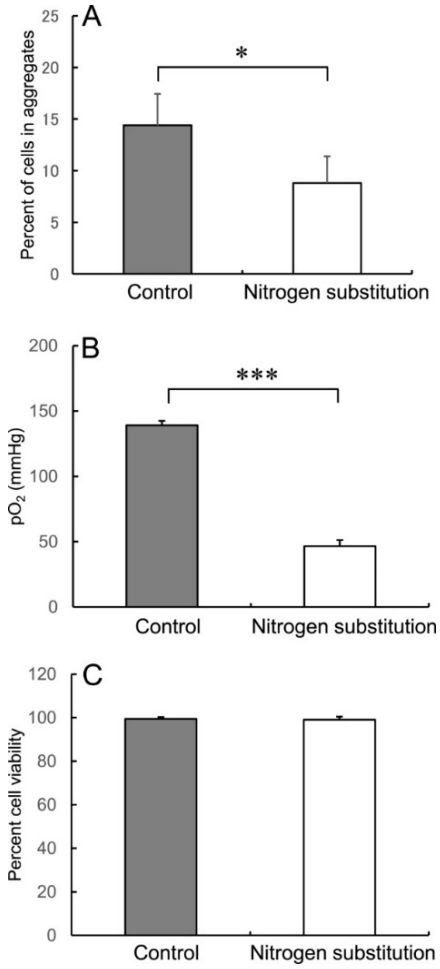

Figure 4.5. Aggregation rate (A), pO_2 in the preservation solution (B), and viability (C) of hADSCs after storage at 25 °C for 24 h in LR-3T-5D in tubes with or without (control) nitrogen gas in the head space. Data are presented as the mean ± SD (n = 5). Statistical analysis was performed using two-tailed non-paired *t*-test: ∗$p < 0.05$, ∗∗∗$p < 0.001$.

4.4 Discussion

MSCs are often administered intravascularly for cell therapy purposes [Terashvili *et al.* 2019, Munir *et al.* 2015, Wyles *et al.* 2015, Trounson *et al.* 2015, Murata *et al.* 2021, Dilogo *et al.* 2021, Adas *et al.* 2021], but aggregation can lead to vascular embolization. In the present study, we assessed the effect of various storage conditions on the aggregation of MSCs and provide suggestions regarding how to avoid such aggregation. A high rate of hADSC aggregation was observed when cells were stored in LR-3T-5D at 25 °C for 24 h. Similarly, when human bone marrow-derived mesenchymal stem cells (hBM-MSCs) were stored for 24 h at 25 °C, the aggregation was observed in LR-3T-5D (data not shown). Regardless of origin, MSCs are adhesive cells. Low-adhesive containers were used in storage experiments to avoid adherence to containers and increase the number of cells recovered. On the other hand, MSCs also adhere to each other and form spheroids when cultured in low-adhesion containers [Cesarz *et al.* 2016]. In this experiment, MSCs may have adhered to each other during storage, causing aggregation. In contrast, the aggregation rate of hADSCs stored at 5 °C for 24 h was similar to the pre-storage rate. Typically, cells are stored at low temperatures to inhibit cell metabolism and prevent cell death due to ATP depletion [McLaren *et al.* 2003]. Moreover, the expression of membrane proteins such as cadherins is reportedly important for MSC adhesion [Wuchter *et al.* 2007]. Although the mechanism of storage-associated cell aggregation remains unclear, aggregation may be inhibited by the suppression of membrane protein function at low temperatures.

In the present study, the aggregation rate and viability of cells stored at 25 °C for up to 6 h were comparable between cells stored in LR versus LR-3T-5D. However, when the cells were stored for 24 h at 25 °C, both the aggregation rate and viability of

cells stored in LR were lower compared with cells stored in LR-3T-5D. Similar results were observed for cells stored at 5 °C for 24 h. Colony-forming assays have clearly shown that cells with low viability also exhibit low rates of adhesion and proliferation [Fujita *et al.* 2021]. Our observations also suggest that the decrease in cell viability during storage plays a role in lowering the rate of cell aggregation. In addition, LR-3T-5D contains dextran 40 in order to float the cells in suspension [Fujita *et al.* 2020]. Dextran coatings reportedly enhance the adhesion of BM-MSCs to sponge scaffolds [Togami *et al.* 2014]. Dextran 40 may have been involved in promoting aggregation.

In the present study, we show that the pO_2 of the preservation solution is related to the rate of cell aggregation after preservation. The following three conditions can be taken to reduce the pO_2 of the solution and inhibit aggregation without reducing cell viability. First, as shown in Figure 4.3A and B, increasing the volume of the preservation solution lowers the pO_2 in the suspension and the cell aggregation rate. This is a reasonable method that requires no any special manipulation or preparation of a large number of cells. We hypothesize that the pO_2 in the solution decreases because the volume of the air layer in the tube and the gas exchange efficiency from the solution surface decrease when the volume of solution increases. Second, as shown in Figure 4.4A and B, increasing the amount of the preserved cell lowers the pO_2 in the suspension and the cell aggregation rate. This is a reasonable method that requires no any special manipulation and without changing the suspension volume. Preserving cells as higher-density suspensions decreases the pO_2, presumably as a result of increased oxygen consumption due to the increased number of cells in the suspension. Third, as shown in Figure 4.5A and B, replacing the head space in the sealed test tube with nitrogen gas was shown to decrease the pO_2 in the solution and the cell aggregation rate. This method is useful when the number of cells and the volume of the suspension

should not be changed. It is assumed that this effect inferred as resulting from the equilibration of oxygen in the solution with the nitrogen in the head space.

In studies using cancer cells, hypoxia has been shown to suppress the expression of cell surface proteins such as cadherins [Zhang *et al.* 2015, Duś-Szachniewicz *et al.* 2018]. In the present study, nitrogen gas replacement significantly inhibited cell aggregation by reducing the pO_2 of the preservation solution to 46.6 mmHg after 24 h of storage. The pO_2 in normal adipose tissue is approximately 50 mmHg, and one study suggests adipose tissue-derived MSCs are inherently hypoxia tolerant, with oxygen levels as low as 1% having no effect on survival [Suga *et al.* 2010]. Indeed, in the present study, the viability of hADSCs was not affected even under nitrogen gas replacement conditions, suggesting that hypoxia itself not only inhibits cell aggregation but also poses a low risk to the cells.

On the other hand, studies with vascular endothelial cells and human umbilical vein endothelial cells have shown that exposure to reactive oxygen species (ROS) results in altered expression of cell surface proteins and increased adhesion [Patel *et al.* 1991, Sellak *et al.* 1994]. Although it remains unclear which factors mediate the effects of ROS on cell adhesion, lowering the pO_2 in the suspension may suppress ROS generation. Perhaps the three preservation conditions presented here suppress the generation of ROS by lowering pO_2 and inhibit the aggregation of the preserved cells by controlling changes in the expression of cell surface proteins.

4.5 Conclusions

In the present study, high cell aggregation rates were observed when hADSCs were stored in LR-3T-5D for 24 h at 25 °C, although their viability was maintained. Our data suggest that cell aggregation can be reduced by lowering the pO_2 of the preservation solution by increasing the volume and cell density as well as by nitrogen gas replacement.

5. Development and characterization of islet-derived mesenchymal stem cells from clinical grade neonatal porcine cryopreserved islets

5.1 Introduction

Mesenchymal stem cells (MSCs) exhibit various effects, including pluripotent differentiation, immunosuppression, and extracellular matrix remodeling, and have many clinical applications [Berry *et al.* 2019, Yokota *et al.* 2019, Staff *et al.* 2019, Moll *et al.* 2019, Qu *et al.* 2022]. Several MSC-derived drugs are currently available on the market [Konishi *et al.* 2016, Gibbons. 2015, Scott. 2018]. In addition to their therapeutic effects, MSCs enhance the therapeutic effects of target cells when co-cultured or co-transplanted [Alzebdeh *et al.* 2017, Wang *et al.* 2018, Sordi *et al.* 2010], Further research into their therapeutic applications is underway. The demand for MSCs as sources of cell therapy is expected to increase in the future because, unlike embryonic stem cells, they do not pose ethical concerns and have fewer risks associated with gene transfer than induced pluripotent stem cells. However, securing sources for therapeutic applications of MSCs presents a challenge. Cell banks are necessary for the expansion of MSC therapy; however, securing sufficient allograft donors is difficult [Lechanteur *et al.* 2016]. Using autologous MSCs from a patient is also possible; however, there are safety issues associated with the collection of peripheral blood, bone marrow [Fujimoto *et al.* 2020], and adipose tissue [Kaoutzanis *et al.* 2017].

Pigs are physiologically and anatomically similar to humans. Furthermore, a stable supply of pigs is available. Recently, organ transplants from pigs to humans have been performed and medical use of pigs is expected to increase [Griffith *et al.* 2022,

Montgomery *et al.* 2022]. By the way, controlling the risk of infectious diseases between humans and animals is also important for the medical use of pigs. Therefore, we focused on clinical-grade pigs with controlled infection risk as a source of MSCs for clinical applications. Clinical-grade pigs are designed pathogen-free pigs that have been created, assessed, and maintained in an isolated barrier facility as mentioned when discussing xenotransplantation regulations [Schuurman *et al.* 2015]. Previously, we isolated and cultured mesenchymal stem cells from clinical grade neonatal porcine bone marrow (npBM-MSCs) and characterized them [Nishimura *et al.* 2019]. Furthermore, we have confirmed the therapeutic efficacy of porcine-derived MSCs by transplanting npBM-MSCs into mice models of ischemic limb disease and diabetic wound healing [Yamada *et al.* 2021, Yamada *et al.* 2022]. The therapeutic application of these cells are being investigated.

MSCs can be produced from various tissues within the body, and they differ from the derived tissues in their proliferative and secretory characteristics [Ruetze *et al.* 2014]. Understanding the differences in the characteristics of MSCs depending on the derived tissue is crucial to determine the therapeutic effects of MSCs and their influence on co-culture with other cells.

Several studies have examined the use of MSCs in diabetes treatment, including bone marrow-derived MSC co-transplantation [Wang *et al.* 2018]. Of note, we previously performed encapsulated porcine islet transplantation for the treatment of unstable type 1 diabetes mellitus in the clinical setting [Matsumoto *et al.* 2016, Nishimura *et al.* 2017]. We assume that co-transplantation of porcine islets and porcine islet-derived MSCs could improve the efficacy of clinical islet xenotransplantation. Furthermore, since we are able to create clinically available porcine islets, MSCs derived from the clinically applicable islets have advantages for regulatory approval. On

the other hand, for regulatory approval, it is required to provide standard characterization of MSCs; therefore, in this study, we characterized our islet-derived MSCs.

To establish MSCs from tissue, including islets, the adhesion of the MSCs to the culture dish is an essential step, which requires several days of labor. By establishing MSCs from cryopreserved tissue, the procedure can be performed at any time, resulting in increased convenience. Although there are many studies on islet cryopreservation, most of them focus on evaluating the functionality of cryopreserved islets for transplantation [Kojayan *et al.* 2018, Zhan *et al.* 2022, Marquez-Curtis *et al.* 2022] and there is limited information on the use of cryopreserved islets as a source of MSCs.

In this study, we investigated the establishment and characterization of MSCs from cryopreserved clinical grade neonatal porcine islets, which may serve as a source of therapeutic MSCs.

5.2 Materials and methods

5.2.1 Animals

The study was approved by the Committee for the Care and Use of Laboratory Animals of Otsuka Pharmaceutical Factory, Inc. (Naruto, Japan). Clinical grade neonatal pigs were provided by Spring Point Project (New Richmond WI, USA), and non-clinical grade neonatal pigs were obtained from Kadoi Ltd (Ibaraki, Japan) (Table 5.1). The pigs were euthanized by bleeding from the abdominal aorta under anesthesia conditions and their pancreases were procured using a sterile technique [Hillberg *at al*. 2013]. Pancreas were preserved using ice cold ET-Kyoto solution (ETK, Otsuka

Pharmaceutical Factory, Inc.). Pancreas from non-clinical grade neonatal pigs were shipped to Otsuka Pharmaceutical Factory, Inc. Additionally, the cold preservation time was 3 h. The procured pancreas of 12 piglets (clinical grade) and eight piglets (non-clinical grade) were processed as previously described to isolate islets [Matsumoto *et al.* 2002]. A clinical grade neonatal pig islet was preserved with ice-cold modified Dilution Solution (Corning Incorporated, NY, USA) and shipped to Otsuka Pharmaceutical Factory, Inc. (Naruto, Japan) for analysis. The cold preservation process took approximately 4 days. We determined the Islet yield using 2 mg/mL dithizone staining (Sigma Chemical Co., St. Louis, MO, USA) under optical reticule to determine a standard number of islet equivalents (IEQ, diameter standardized to 150 μm) [Matsumoto *et al.* 2014].

Table 5.1. Information on neonatal pigs.

	npBM-MSC†	npISLET-MSC‡		
Lot No.	N170926	N170710	N171121	SPP34
Strain	LWW	LWW	LWW	Landrace
Number of animals	1	8	8	12
Age (day)	14	14	14	15 (n=6) 16 (n=6)
sex	Male (n=1)	Male (n=4) Female (n=4)	Male (n=5) Female (n=3)	Male (n=7) Female (n=5)
grade	Non-clinical	Non-clinical	Non-clinical	Clinical
body weight (kg)	3.2	3.0-3.6	3.6-4.6	4.5-6.6
Freeze date of islet	-	2017/7/13	2017/11/14	2017/11/6
Thawing date of islet	-	2017/7/18	2022/6/6	2022/5/31
Freeze date of MNCs§	2017/9/26	-	-	-
Thawing date of MNCs	2017/09/29	-	-	-
Freezing period (day)	3	0 and 5	1663	1666

† neonatal porcine bone marrow derived from mesenchymal stem cells
‡ neonatal porcine islet derived from mesenchymal stem cells
§ mononuclear cells

5.2.2 Cryopreservation of islets of neonatal pigs

The islets were collected at modified RPMI in a 50 mL tube. The islet suspension was static, the islets were sedimented, and the supernatant was removed. The isolated islets were resuspended at 6,000 IEQ/mL with Cellstor-S (lactated Ringer's solution with 3% trehalose and 5% dextran 40) (Otsuka Pharmaceutical Factory, Inc. Tokushima, Japan) containing 10% Dimethyl Sulfoxide (DMSO). Each cryovial contained 1 mL of isolated islets. The cryovials were placed in a BICELL (Nihon Freezer Co., Ltd., Tokyo, Japan) and frozen at −80°C for 24 h before being transferred to liquid nitrogen tanks for long-term storage.

5.2.3 Thawing and culturing of islets to create npISLET-MSCs

The islets (6,000 IEQ) in a cryovial were rapidly thawed in a 37 °C water bath, and 30 mL of MSC culture medium was gently added to the thawed cell suspension. Subsequently, it was centrifuged for 1 min at 210 × *g* at approximately 22 °C. The supernatant was removed, and 8 mL of MSC culture medium was gently added to the pellet. The pellet was gently resuspended in an MSC culture medium by pipetting up and down. The islets (2,000 IEQ/well) were plated on a 6-well plate in 2 mL of MSC culture medium. The same MSC culture medium was used for both clinical and non-clinical grades of npISLET-MSCs: MEM α (12571-063, Gibco) containing 10% FBS, 100 U/mL penicillin, 100 μg/mL streptomycin, and 1 ng/mL human fibroblast growth factor-basic (hBFGF, F0291, Sigma-Aldrich). The 6-well plate was placed in a CO_2 incubator and incubated at 37 °C, 5% CO_2, and 90% humidity. Clinical grade npISLET-MSCs and non-clinical grade npISLET-MSCs reached approximately 50%–

80% confluence after 3 days. Clinical-grade npISLET-MSCs were established from islets cryopreserved for more than 4 years (Figure 5.1).

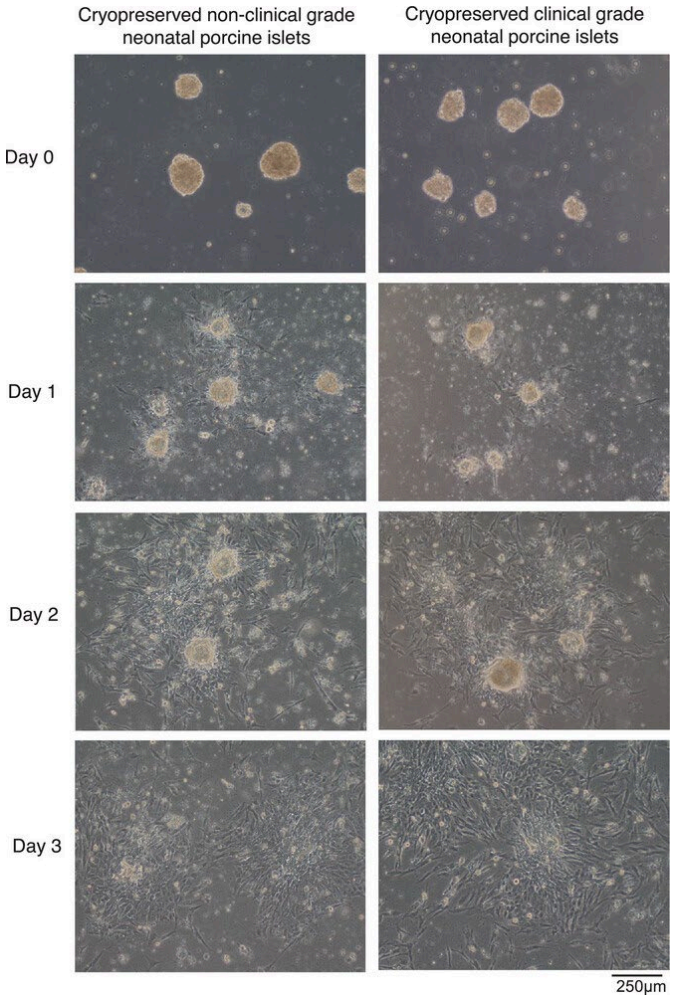

Figure 5.1. Micrographs of cultured cryopreserved clinical grade and non-clinical grade neonatal porcine islets (A). Islets cryopreserved for more than 4 years in Cellstor-S containing 10% DMSO were used. Islet (2,000 IEQ/well) was cultured by plating 6-well plates with 2 mL MSC culture medium.

5.2.4 Passage of npISLET-MSCs

The cells from the 6-well plates were collected and replated into 75 cm^2 flasks after reaching approximately 50%–70% confluence. We washed the cells with 2 mL

Phosphate buffered saline without calcium and magnesium ions (PBS (-)) and added 320 μL of 0.25% trypsin per well. The cells were kept in the incubator for 3 min at 37 °C. After the cells were detached, trypsin was neutralized with 1,680 μL of MSC culture medium per well. The cell suspensions from four wells were collected into a 50 mL tube, and 32 mL (8 mL × 4 wells) of MSC culture medium was added. The cell suspensions were centrifuged for 5 min at 500 × *g* at approximately 22 °C. The cell pellet was resuspended in an MSC culture medium. The numbers of total and dead cells were counted. The cell suspensions (3×10^5–6×10^5 total cells/flask) were replated into 75 cm^2 flasks in a 20 mL MSC culture medium. The 75 cm^2 flasks were placed in an incubator; the incubated cells were termed as passage 1 cells.

5.2.5 Cryopreservation of npISLET-MSCs

If the npISLET-MSCs created are not used immediately, they are cryopreserved for future use. We washed the cells with 8 mL PBS (-) and added 2.4 mL of 0.25% trypsin per 75 cm^2 flask. The cells were kept in the incubator for 3 to 5 min at 37 °C. The trypsin was neutralized with 12.6 mL of MSC culture medium per 75 cm^2 flask after the cells were detached. The cell suspensions were collected in a 50 mL tube. The cell suspensions were centrifuged for 5 min at 500 × *g* at approximately 22 °C. The isolated npISLET-MSCs were resuspended at 3×10^6–6×10^6 cells/mL with Cellstor-S containing 10% DMSO or 4% propylene glycol. Approximately 1 mL of isolated npISLET-MSCs were placed in each cryovial. The cryovials were placed in a BICELL frozen at −80 °C for 24 h and then transferred to a liquid nitrogen tank for long-term storage.

5.2.6 Thawing and culturing of npISLET-MSCs

The npISLET-MSCs in a cryovial was rapidly thawed in a 37 °C water bath. To the thawed cell suspension, 10 mL of MSC culture medium was gently added. Furthermore, it was centrifuged for 5 min at 500 × *g* at approximately 22°C. The supernatant was removed, and 10 mL of MSC culture medium was gradually added to the pellet. The pellet was gently resuspended in an MSC culture medium by pipetting up and down. We counted the number of total and dead cells. The cell suspensions (3×10^5 total cells/flask) were seeded into 75 cm^2 flasks in a 20 mL MSC culture medium. The 75 cm^2 flask was placed in the CO_2 incubator and incubated at 37 °C, 5% CO_2, and 90% humidity. Both clinical grade npISLET-MSCs and non-clinical grade npISLET-MSCs were approximately 90% confluent after 4 days of culture. When the cells reached 90% confluence, they were collected and replated into 75 cm^2 flasks or used for each experiment. We washed the cells with 8 mL PBS (-) and added 2.4 mL of 0.25% trypsin per 75 cm^2 flask. The cells were kept in the incubator for 3 to 5 min at 37 °C. Following the detachment of the cells, trypsin was neutralized with 12.6 mL of MSC culture medium per 75 cm^2 flask. The cell suspensions were collected in a 50 mL tube. The cell suspensions were centrifuged for 5 min at 500 × *g* at approximately 22 °C, and the supernatant was aspirated. The cells were suspended in an MSC culture medium and used for each experiment.

5.2.7 Preparation, Thaw, culture, and passage of npBM-MSCs

The preparation, thaw, culture, and passage of npBM-MSCs were performed according to our previous study [Nishimura *et al.* 2019].

5.2.8 Cell viability

Cell viability was determined manually with a plastic cell counting plate (OneCell Counter, Fine Plus International Ltd., Kyoto, Japan) under a microscope by trypan blue staining. Cell viability was calculated according to the formula below:

Cell viability [%] = (Total cell count - dead cell count) / (Total cell count) × 100.

Alternatively, cell viability was determined using a NuceloCounter NC-202 (M&S TechnoSystems, Inc.).

5.2.9 Cell proliferation assay

Cryopreserved cells were used after one or more passages. To plot the growth curve, passage-5 cells of non-clinical grade npBM-MSC and passage-3 cells of non-clinical and clinical grade npISLET-MSCs were plated at a density of 5,000 cells/cm^2 (1.25×10^5 cells/flask) in a 25 cm^2 flask. The MSC culture media were changed every 3 days. The same flasks were trypsinized, and the total number of cells was counted at 1, 2, 4, and 8 days. The growth curve was then plotted using the cell counting data. The doubling time (DT) was calculated using the following formula:

Doubling time (h) = $[\{(T-T_0)(\log_2)\}/(\log N - \log N_0)]$,

where T is the time (h), N is the cell count, and T_0, N_0 is the initial value.

5.2.10 Analysis of cell size

Analysis of cell size was performed at the end of the passage using a NuceloCounter NC-202.

5.2.11 Quantification of cell surface marker

To examine the cell surface immunophenotypes and forward scatter, 1×10^7 cells/mL (20 to 100 μL) in Stain Buffer with FBS (BD Biosciences, San Jose, CA, USA) were incubated on ice for 45 min. The cells were incubated with Alexa Fluor 647-labeled antibody against pig CD29 (BD Biosciences, San Jose, CA, USA; Clone NaM160-1A3); purified mouse against pig SLA-DR (BD Biosciences; Clone 1053H2-18) and FITC-labeled against mouse IgG2a (BD Bioscience; Clone R19-15); phycoerythrin (PE)-labeled antibodies against rat CD31 (BD Biosciences; Clone TLD-3A12), against mouse CD44 (GeneTex, Inc., Irvine, CA, USA; Clone MEM-263), and against human CD90 (BD Biosciences; Clone 5E10); and Alexa Fluor 488-labeled antibodies against human CD34 (Abcam, Cambridge, England; Clone EP373Y) crossing to pig or the respective isotype controls (BD Biosciences, Abcam). After washing, the labeled cells were analyzed using a Gallios Flow Cytometer (Beckman Coulter, Indianapolis, IN, USA).

5.2.12 Adipogenic and osteogenic differentiation

Cryopreserved cells were used after one or more passages. We induced the adipogenic and osteogenic differentiation of clinical grade npISLET-MSCs. Induction of

adipogenic differentiation was performed according to Poietics human mesenchymal stem cells — Adipogenic assay procedure (Lonza Walkersville, Inc.), and evaluated using Oil Red staining. Induction of osteogenic differentiation was performed according to the procedure manual of Poietics human mesenchymal stem cells — Osteogenic assay procedure (Lonza Walkersville, Inc.) and evaluated using Alkaline Phosphatase Staining kit (AK20, Cosmo Bio Co., Ltd.).

5.2.13 Colony forming unit (CFU) assay

Cryopreserved cells were used after one or more passages. Cells were plated at a density of 315 cells in a 21 cm^2 culture dish (30 cells/cm^2). The MSC culture media were changed at day 3 and 6. After culturing for 8 days, adherent cells were washed twice with 4 mL PBS and fixed with 4 mL ice-cold methanol for 15 min at 4 °C. To visualize colonies, cells were stained with 4 mL Giemsa diluted 1:19 with phosphate buffer for 30 min at room temperature and washed twice with H_2O. The number of colonies with more than 50 cells was counted. The colony-forming efficiency of cells was calculated by dividing the number of colonies per dish by the number of cells (315) seeded per dish.

5.2.14 Analysis and statistics

Data are presented as the mean ± standard deviation (SD). Statistical analyses were performed using two-tailed tests, consisting of either Tukey's test or a non-paired Student's t-test, and a significance level of less than 5% was considered statistically significant. Data were analyzed using SAS 9.4 (SAS Institute, Inc., Cary, NC, USA).

5.3 Results

5.3.1 Differences to establish neonatal porcine islet-derived MSC with and without cryopreservation

Fresh and cryopreserved non-clinical grade neonatal porcine islets were treated with Cellstor-S containing 10% DMSO for 5 days to prepare MSCs. The fresh islets were seeded in 6-well plates, and incubated at 37 °C, 5% CO_2, and 90% humidity. Cryopreserved islets were rapidly thawed, washed with medium, seeded in 6-well plates and incubated at 37 °C, 5% CO_2, and 90% humidity. Fresh islets and cryopreserved islets are both suspended in an MSC culture medium and seeded, resulting in cell growth (Figure 5.2A). It was found that both groups had a high level of positive expression of MSC surface markers such as CD29, CD44, and CD90 (Figure 5.2B).

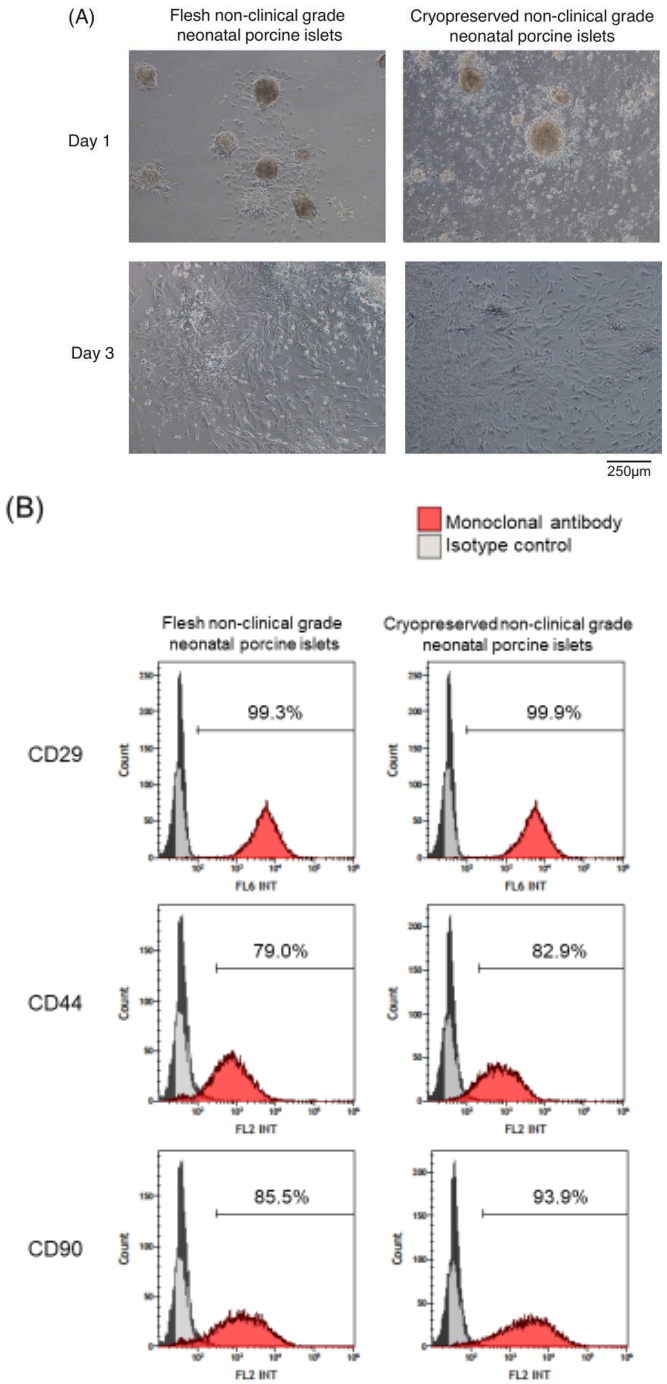

Figure 5.2. Micrographs of cultured fresh and cryopreserved islets (A). Fresh and cryopreserved non-clinical grade neonatal porcine islets were treated with Cellstor-S containing 10% DMSO for 5 days to prepare MSCs). Islets (2,000 IEQ/well) were cultured on 6-well plates with 2 mL MSC culture medium. Immunophenotypes on the cell surface of npISLET-MSCs (Passage 2) as analyzed using flow cytometry (B). Cells are prominently positive for CD29, CD44, and CD90. Data obtained from a representative example (n = 1) is shown.

5.3.2 Comparison of growth kinetics of non-clinical grade npBM-MSC, non-clinical grade npISLET-MSC, and clinical grade npISLET-MSC

MSCs were seeded at 5,000 cells/cm^2 (1.25 × 10^5 cells/flask) in a 25 cm^2 flask, and both cells reached approximately 80% confluence on day 4 and 100% confluence on day 6. The calibrated growth curve was plotted for the non-clinical grade npBM-MSCs, non-clinical grade npISLET-MSCs, and clinical grade npISLET-MSCs (Figure 5.3A). Cell counts for non-clinical-grade npBM-MSCs, non-clinical-grade npISLET-MSCs, and clinical-grade npISLET-MSCs were as follows: day 1 of culture, 2.62 × 10^5 ± 0.96, 1.37 × 10^5 ± 0.13, and 1.26 × 10^5 ± 0.12 cells/flask, respectively; day 2 of culture, 5.97 × 10^5 ± 0.92, 3.56 × 10^5 ± 0.36, and 3.68 × 10^5 ± 0.36 cells/flask, respectively; day 4 of culture, 17.29 × 10^5 ± 1.15, 11.23 × 10^5 ± 1.32, and 12.58 × 10^5 ± 1.07 cells/flask, respectively; day 6 of culture, 47.73 × 10^5 ± 4.09, 24.09 × 10^5 ± 2.41, and 30.22 × 10^5 ± 2.41 cells/flask, respectively; and day 8 of culture, 46.78 × 10^5 ± 2.52, 26.97 × 10^5 ± 2.27, and 30.34 × 10^5 ± 2.36 cells/flask, respectively. Non-clinical-grade npBM-MSCs had significantly higher cell counts at all points compared to non-clinical-grade npISLET-MSCs and clinical-grade npISLET-MSCs (day 1: p = 0.030 and 0.020, day 2: p = 0.001 for both, days 4, 6, 8: all p < 0.001, respectively). On day 6, the number of cells was significantly higher in clinical-grade npISLET-MSCs than in non-clinical-grade npISLET-MSCs (p = 0.048). DT of non-clinical grade npBM-MSCs, non-clinical grade npISLET-MSCs, and clinical grade npISLET-MSCs were 25.7 ± 1.1, 30.5 ± 1.8, and 28.9 ± 1.0 h, respectively (Figure 5.3B). There were no significant differences between the DT of non-clinical grade npISLET-MSCs and clinical-grade npISLET-MSCs. The DT of non-clinical-grade npBM-MSCs was significantly shorter than that of

non-clinical-grade and clinical-grade npISLET-MSCs ($p = 0.002$ and $p = 0.021$, respectively).

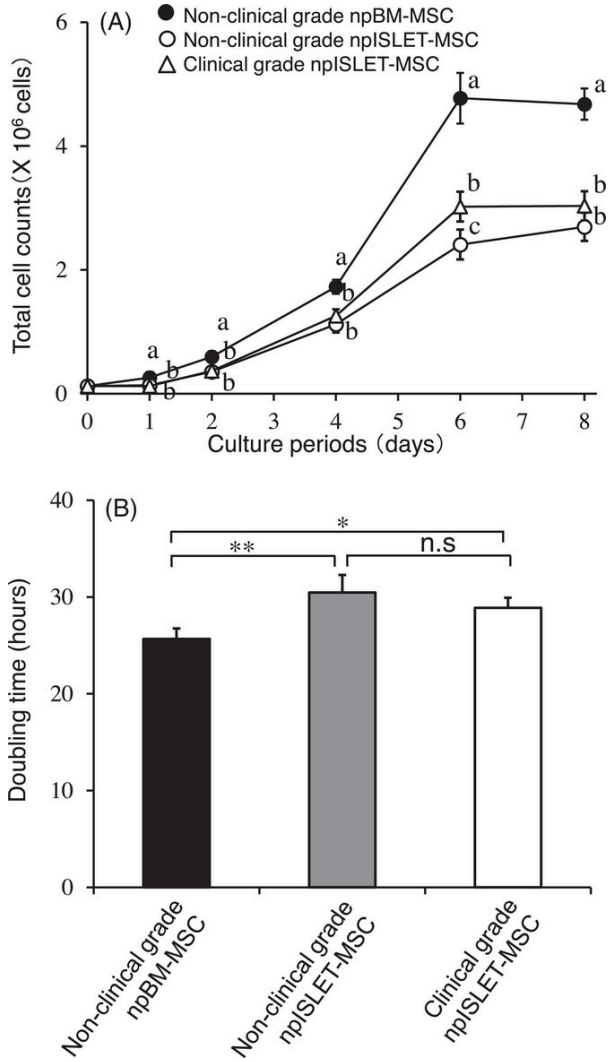

Figure 5.3. Growth curves for non-clinical grade npBM-MSCs (solid circles), non-clinical grade npISLET-MSCs (open circles), and clinical grade npISLET-MSCs (triangle) (A), and doubling time (DT) (B). To plot the growth curve, cells from passages 3 to 5 that were cultured in a 75 cm^2 flask without a gelatin coat were plated at a density of 5,000 cells/cm^2 (1.25×10^5 cells/flask) in a 25 cm^2 flask without gelatin coat. The corresponding flasks were trypsinized, and the total number of viable and dead cells after 1, 2, 4, 6, and 8 days was counted. The growth curve was then plotted using the cell counting data. The DT was calculated from total cell counts immediately and 48 h after inoculation. Results are shown as mean ± SD values ($n = 4$). A: Different letters indicate significant differences by Tukey's test ($p < 0.05$). B: *$p < 0.05$, **$p < 0.01$.

5.3.3 Comparison of cell size of non-clinical grade npBM-MSC, non-clinical grade npISLET-MSC, and clinical grade npISLET-MSC

The mean diameters of non-clinical grade npBM-MSCs, non-clinical grade npISLET-MSCs, and clinical grade npISLET-MSCs were 15.9 ± 0.3, 18.5 ± 0.3, and 18.8 ± 0.5 μm, respectively (Figure 5.4). There were no significant differences between the cell size of non-clinical grade npISLET-MSCs and clinical grade npISLET-MSCs. The cell size of non-clinical grade npBM-MSCs was significantly smaller than that of non-clinical and clinical grade npISLET-MSCs (p <0.001).

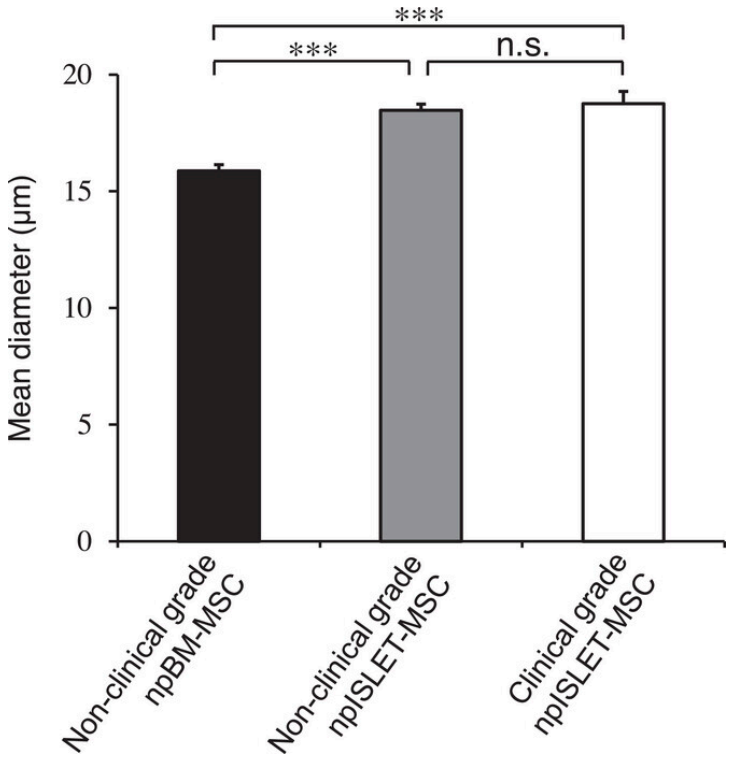

Figure 5.4. Mean diameters of non-clinical grade npBM-MSCs, non-clinical grade npISLET-MSCs, and clinical grade npISLET-MSCs. MSCs from passages 2 to 3 were used. The results of MSCs are shown as mean ± SD (n = 4). The diameter of non-clinical-grade npBM-MSCs is significantly smaller than that of non-clinical grade npISLET-MSCs and clinical grade npISLET-MSCs. Tukey's test ***p <0.001.

5.3.4 Immunological surface phenotypes of non-clinical grade npBM-MSC, non-clinical grade npISLET-MSC, and clinical grade npISLET-MSC

In all groups, positive MSC surface markers, such as CD29, CD44, and CD90, were highly expressed (Figure 5.5A). Negative surface markers, such as the endothelial marker CD31 and hematopoietic marker SLA-DR (a marker of swine corresponding to major histocompatibility antigen HLA-DR of human cells), were absent in all groups (Figure 5.5B). Hematopoietic marker CD34 of MSC negative marker was expressed slightly (9.1%, 5.8%, and 6.0%) in non-clinical grade npBM-MSC, non-clinical grade npISLET-MSC, and clinical grade npISLET-MSC, respectively (Figure 5.5B).

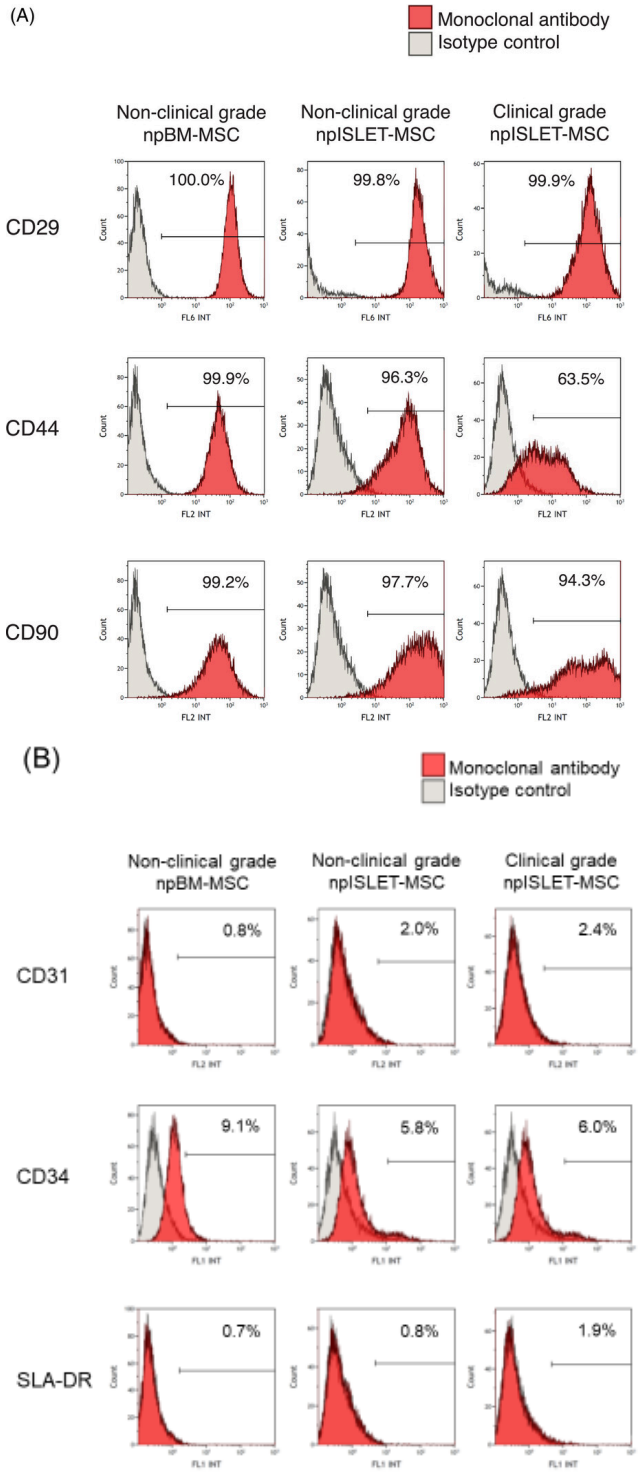

Figure 5.5. Immunophenotypes on the cell surface of MSCs as analyzed using flow cytometry. All cell types are prominently positive for CD29, CD44, and CD90 (A) and negative for the endothelial marker CD31 and hematopoietic markers SLA-DR. Additionally, the cells are weakly positive for the hematopoietic marker CD34 (B). Data obtained from a representative example (n = 1) are shown.

5.3.5 Adipogenesis and osteogenesis of clinical grade npISLET-MSC

The Oil Red stain (Figure 5.6A) and alkaline phosphatase stain (Figure 5.6B) were both positive. Therefore, our clinical-grade npISLET-MSCs differentiated into adipocytes and osteocytes.

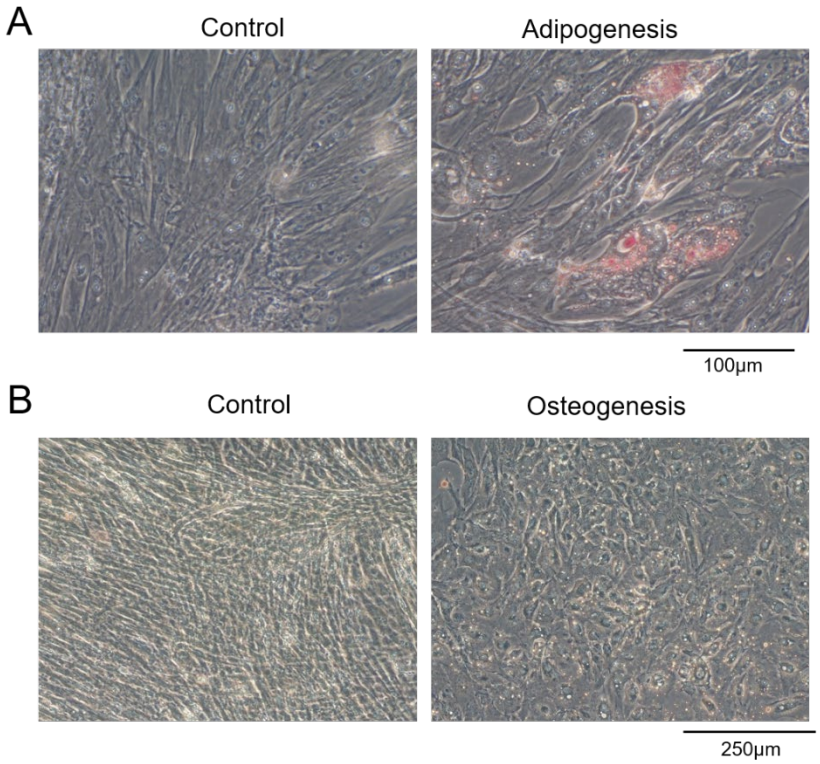

Figure 5.6. Differentiation potential of clinical grade npISLET-MSCs. Induction of adipogenic differentiation was evaluated using Oil Red staining (A). Induction of osteogenic differentiation was evaluated using alkaline phosphatase staining (B).

5.3.6 CFU assay of non-clinical grade npBM-MSC and clinical grade npISLET-MSC

Colony-forming efficiency of cells of non-clinical grade npBM-MSCs and clinical grade npISLET-MSCs was 17.6 ± 2.8% and 21.7 ± 2.5%, respectively. Furthermore, there were no significant differences between the two groups. (Figure 5.7).

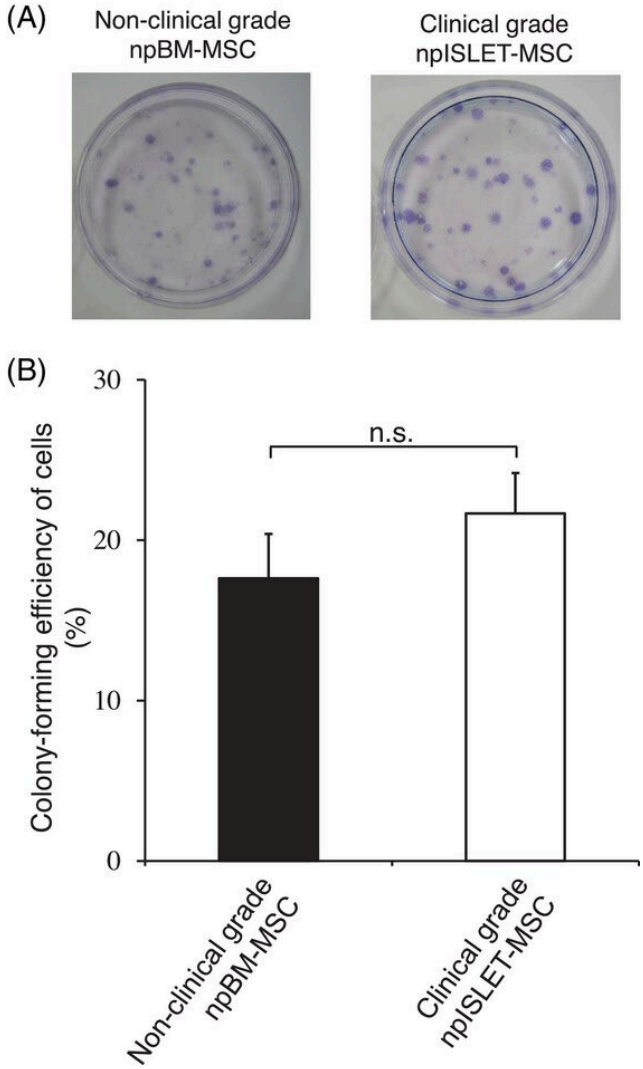

Figure 5.7. Comparison of non-clinical grade npBM-MSCs and clinical grade npISLET-MSCs using Colony Forming Unit (CFU) assay. Representative images (A). Colony-forming efficiency of cells (%) in CFU assay (B). There were no significant differences between the two groups (n=4, student's t-test).

5.4 Discussion

In addition to bone marrow [Fu *et al.* 2019] and fat [Cai *et al.* 2020], various other tissues, including pancreatic islets [Davani *et al.* 2007], can be used to establish MSCs. In this study, we demonstrate for the first time that MSCs can be established from islets cryopreserved for a period of more than 4 years. Islets are difficult to freeze, and after thawing, their functions such as viability and insulin secretion are reduced [Kojayan *et al.* 2018]. Recent studies have shown that islets can be frozen and thawed by improving cryoprotectants and cryo methods [Zhan *et al.* 2022, Marquez-Curtis *et al.* 2022]. Generally, islets are not cryopreserved in clinical protocols to avoid loss of function [Ricordi *et al.* 2016, Ito *et al.* 2022]. In contrast, MSCs are relatively resistant to freezing injury and have minimal loss of function and viability after thawing [Marquez-Curtis *et al.* 2015]. Despite the possibility that the cryopreserved islets used in this study may have impaired insulin secretion and other functions, we speculate that this had an insignificant effect on the stem cells included in this study and thus, did not adversely affect the establishment of MSCs. In this study, MSCs were established from islets using a more general and simple method of slow freezing and thawing in a warm bath at 37°C. Although pig islets have a fragile constitution [Salama *et al.* 2017], we have demonstrated that they can be used to establish MSCs at any time, even after being frozen for more than 4 years.

In the clinical application of porcine MSCs, unlike human MSCs, there should be less risk related to securing donors [Lechanteur *et al.* 2016, Fujimoto *et al.* 2020, Kaoutzanis *et al.* 2017]. However, manufacturing under Good Manufacturing Practice (GMP) conditions is required. Clinical-grade npISLET-MSCs also need to be investigated using GMP-compliant materials in the future, as is being done for the GMP

manufacturing of human islet MSCs [Thirlwell *et al.* 2020]. It is also known that various factors in the production of MSCs, such as source tissue, isolation protocols, media composition, and pre-treatment, affect the chemokine expression, immunomodulatory capacity, and therapeutic efficacy of MSCs [Cuesta-Gomez *et al.* 2021]. For npISLET-MSCs, there is insufficient information about secreted products, chemokines, and other characteristics that affect their therapeutic effect. There may be some characteristics related to their being derived from neonatal pigs rather than adults pigs, as observed in the bone marrow [Nishimura *et al.* 2019]. In the future, these characteristics should be clarified, and appropriate quality control parameters should also be established. Furthermore, MSCs are known to change their proliferation rate, surface markers, and differentiation potential with passaging [Yang *et al.* 2018]. Once quality control parameters have been determined, changes in character after passaging should be observed for npISLET-MSCs. We believe that use of pigs can allow production of MSCs on a larger scale than humans because there do not exist the same limitations associated with securing donors. It is important to establish MSCs with the same properties even from different batches in large-scale production. We have also isolated islets from another individual clinical-grade pig and established MSCs. A detailed study will be conducted in the future, but at least the growth curve of cell proliferation was similar to that of npISLET-MSCs, but not BM-MSCs (data not shown). As mentioned earlier, it is necessary to maintain as stable a source of MSCs as possible when establishing production protocols and quality control parameters or clinical applications. In this regard, it is notable that the present study showed that porcine islets, the source of MSCs, can be cryopreserved for longer than 4 years, and that the established MSCs can be grown in sufficient quantities.

When MSC surface markers were measured, positive MSC surface markers such

as CD29, CD44, and CD90 were highly expressed in all groups, and negative markers such as CD31 and SLA-DR were not seen. CD34, a marker for hematopoietic stem cells, was weakly detected in all groups. However, it has also been reported that various progenitor cells, including MSCs, may show CD34 positivity [Sidney *et al.* 2014]. The npISLET-MSCs were established from islets after the purification process. Thus, we consider it unlikely that the MSCs were contaminated with hematopoietic stem cells. Clinical grade npISLET-MSCs were positive for CD44 and CD90 staining, but they showed a wider distribution than the other groups. Clinical grade npISLET-MSCs may be heterogeneous, but the number of studies examining this is small at this time, and data should be accumulated in future studies.

In the present study, the differentiation potential of clinical grade npISLET-MSCs was evaluated using a simple staining kit. Alkaline phosphatase staining has been used as a marker for osteoblast differentiation [Linh *et al.* 2016, Aikawa *et al.* 2016]. In addition, alkaline phosphatase staining is also used to detect pluripotent stem cells [Watanabe *et al.* 2021]. Future studies will need to evaluate osteogenesis in combination with other parameters such as osteocalcin antibodies and osterix mRNA expression level analysis. Clinical-grade npISLET-MSCs showed positive oil red staining after induction of adipogenesis. However, a population of MSCs that maintained the morphology of MSCs rather than adipose tissue was also observed. Comparing the differentiation potential of pancreatic and bone marrow-derived MSCs, it has been reported that pancreatic-derived MSCs are less adipogenic than bone marrow-derived MSCs [Cooper *et al.* 2020]. Differentiation data for clinical grade npISLET-MSCs are not yet sufficiently abundant. Therefore, it will be necessary to accumulate more data in the future.

MSCs are known to have different characteristics depending on their derived

tissue. For example, adipose-derived MSCs (AD-MSCs) are more proliferative than BM-MSCs but have inferior osteogenic potential [Ruetze *et al.* 2014]. Moreover, there are differences in the extracellular vesicles secreted by both the MSCs, with those derived from AD-MSCs having a higher influence on angiogenesis, whereas those derived from BM-MSCs contributing to the promotion of proliferation [Pomatto *et al.* 2021]. Several characteristics of pancreatic/islet-derived MSCs have also been reported. The pattern of chemokines and pro-regenerative factors in islet-derived MSCs is similar to that of BM-MSCs, and they have been shown to have immunomodulatory properties such as that of suppressing T cell proliferation in vitro [Thirlwell *et al.* 2020]. Islet-derived MSCs do not express insulin; however, compared to BM-MSCs, their level of histone modification of the insulin gene is closer to that of islets [Mutskov *et al.* 2007]. Furthermore, some reports have suggested that MSCs established from pancreatic tissue may contribute to islet regeneration by producing more secreted substances involved in vascular development, wound healing, and chemotaxis than BM-MSCs [Cooper *et al.* 2020, Cooper *et al.* 2021].

Additionally, transplantation of islet-derived MSCs into mice results in the differentiation of a number of cells into insulin-secreting cells [Davani *et al.* 2007]. In this study, we found that npISLET-MSCs have a larger average diameter and proliferate less rapidly than npBM-MSCs. The characteristics of ISLET-MSCs, including secretory products and differentiation performance need to be clarified through further research.

It has been reported that MSC co-culture/co-transplantation may enhance the therapeutic effect of cells of interest, such as cells of the liver [Alzebdeh *et al.* 2017] and myocardium [Tachida *et al.* 2016]. Similarly, in pancreatic islets, the inhibition of apoptosis and enhancement of insulin secretory capacity of cultured islets via MSCs-derived exosomes has been reported when co-cultured with Wharton's jelly-

derived MSCs in the umbilical cord [Keshtkar *et al.* 2020]. Furthermore, co-transplantation of BM-MSCs and islets has been reported to significantly reduce the need for postoperative insulin therapy [Wang *et al.* 2018]. We believe that ISLET-MSCs are more effective than other MSCs for islet co-culture/transplantation based on the differentiation potential, the characteristics of cellular secretions, and the gene modification characteristics of ISLET-MSCs mentioned above. In the future, we intend to study islet co-cultivation/transplantation in conjunction with the characterization of the established npSILET-MSCs.

In this study, we developed a method of establishing MSCs from cryopreserved islets of clinical grade pigs. To pursue xenotransplantation therapy using pigs, it is necessary to suppress xeno-immune reactions in addition to managing donor pig hygiene. Thus, pig medical applications are being investigated, including the knockout of multiple antigen genes [Tanihara *et al.* 2021]. Additionally, we have previously reported the establishment of MSCs from pigs lacking the α-Gal antigen [Kikuchi *et al.* 2021]. In the future, we plan to establish MSCs from pigs that are controlled and genetically regulated in a medical environment. This will improve donor supply and ensure stable cell quality for medical applications.

5.5 Conclusions

We have established a method for producing npISLET-MSCs from cryopreserved islets of clinical grade pigs. The preparation of npISLET-MSCs from cryopreserved islets enables a stable supply of cells of the same quality. Clinical grade neonatal porcine cryopreserved islets should be a promising source for future cell therapy using islet-derived MSCs.

6. Development and characterization of Gal KO porcine bone marrow-derived mesenchymal stem cells

6.1 Introduction

Many clinical studies using MSCs derived from human tissues have been conducted, and MSC-derived drugs, such as TEMCELL® HS Inj, has already been in market [Lechanteur *et al.* 2016, Konishi *et al.* 2016]. However, securing adequate cadaveric donors, and the safety of living donors are major issues [Lechanteur *et al.* 2016]. Therefore, we established MSCs from the bone marrow of clinical-grade neonatal porcine [Nishimura *et al.* 2019]. Recently, we demonstrated that the porcine bone marrow-derived MSC could more effectively improve critical ischemic limb disease in rat model compared with murine MSCs [Yamada *et al.* 2021]. Even porcine bone marrow-derived MSC improved the ischemic limb disease in rat model, porcine cells present alpha-Gal which could cause xenogeneic rejection. Elimination of alpha-Gal might improve the efficacy of porcine bone marrow-derived MSC by mitigating xenogeneic rejection of implanted MSCs [Li *et al.* 2014]. Before assessing the efficacy of MSC from alpha-Gal knockout pigs, it is needed to develop the method to create MSCs and characterize the MSCs. Therefore, in this study, we have examined to develop Gal knockout (KO) adult porcine bone marrow-derived MSCs (Gal KO apBM-MSCs) and characterize the MSCs.

6.2 Materials and methods

6.2.1 Animals

All animal care and experimental procedures, including the determination of experimental endpoints, were performed in accordance with the Guidelines for Animal Experiments of Tokushima University. All animals were housed and maintained in accordance with Institutional Animal Care and Use Committee guidelines. The female piglets were maintained for more than 10 months until they became adult pigs and weighed more than 100 kg at the time of sternum collection. Pigs were housed in a temperature-controlled room (25 ± 3 °C) under a 12-h light/12-h dark cycle with free access to water and were provided with commercial feed (JA Nishinihon Kumiai Shiryou, Hyogo, Japan). The health condition of all pigs was observed daily at feeding by the animal husbandry staff under the supervision of an attending veterinarian. In this study, we used two pigs. One pig was Gal KO that was created using CRISPR/Cas9 system as described before [Tanihara *et al.* 2020], and the other pig was wild type (WT). For collecting sternum, adult piglets were euthanized by the intravenous injection of a potassium chloride solution (3 mmol/kg) under deep anesthesia by isoflurane according to the American Veterinary Medical Association Guidelines for the Euthanasia of Animals.

6.2.2 Bone marrow cell collection

Sternum containing bone marrow cells were collected from animals that were euthanized by administration of KCL under general anesthesia with isoflurane.

The sternum was collected and the sternum was cut. While wetting the cut surface of the sternum with a small amount of heparinized PBS, the cut surface of the sternum was scraped off with a scalpel and collected in a 50 mL conical tube containing 40 mL of heparinized PBS. Approximately 0.5 g of bone tissue was collected.

6.2.3 Isolation of WT and Gal KO adult porcine mononuclear cells (WT apMNCs and Gal KO apMNCs)

The bone marrow cells with heparinized PBS were gently suspended, then 10 mL of the cell suspension was poured into four 50 mL tubes (10 mL × 4). A total of 10 mL of the cell suspension was diluted up to 30 mL with PBS. Also, 10 mL of Ficoll–Paque PLUS (GE Healthcare, Japan) was poured into four new 50 mL tubes, and 30 mL of the cell suspension was put into each Ficoll–Paque Plus layer. The tubes were centrifuged at 20 °C for 30 min at 400 × *g* with slow acceleration (one-third of full speed) and the brake off. Three distinct layers were formed. The middle layer of the three layers is the white ring layer. The MSCs were located in the white ring layer. The entire white ring layer was collected into four 50 mL tubes containing 25 mL PBS. The tubes were centrifuged for 7 min at 400 × *g* at room temperature (RT), then the supernatant was removed. Forty milliliters of PBS was added and resuspended, then centrifuged for 7 min at 400 × *g* at RT. The isolated WT apMNCs and Gal KO apMNCs were suspended at MSC basic medium (MEM α without ascorbic acid (A10490-01, Gibco) containing 10% FBS and 100 U/mL penicillin—100 μg/mL streptomycin (P4333, Sigma-Aldrich, St. Louis, MO, USA)).

6.2.4 Culture of WT apMNCs and Gal KO apMNCs to create WT and Gal KO adult porcine bone marrow-derived MSCs (WT apBM-MSCs and Gal KO apBM-MSCs)

The cell suspensions (2×10^6 total cells/well) containing WT apMNCs and Gal KO apMNCs were replated into six-well plate in a 2 mL MSC basic medium. After 3 days culture of MNCs with MSC basic medium, only MSC could attach to the plate. Then, all MSC basic medium was replaced with MSC culture medium (MEM-α (12571-063, Gibco) containing 10% FBS, 100 U/mL penicillin—100 μg/mL streptomycin, 1 ng/mL human fibroblast growth factor-basic (hBFGF, F0291, Sigma-Aldrich) which enabled us to produce MSCs.

The six-well plate was placed in the CO_2 incubator and incubated at 37 °C, 5% CO_2, and 90% humidity. The entire culture medium was replaced once every 3 days. MSC culture medium was used after day 3 to expand the cells. WT apBM-MSCs and Gal KO apBM-MSCs were about 50% confluence at 9 and 12 days, respectively.

6.2.5 Passage of WT apBM-MSCs and Gal KO apBM-MSCs

After the cells reach about 50% confluence, the cells from six-well plate were collected and replated into 75 cm^2 flask. We washed the cells with 2 mL PBS (−) and added 320 μL of 0.25% trypsin per well. The cells were kept in the incubator for 3 min at 37 °C. Once the cells were detached, the trypsin was neutralized with 1,680 μL of MSC culture medium per well. The cell suspensions were collected into a 50 mL tube, and 16 mL (8 mL × 2 wells) MSC culture medium was added. The cell suspensions were centrifuged for 5 min at 500 × *g* at RT. The cell pellet was resuspended in MSC culture

medium. The numbers of total and dead cells were counted. The cell suspensions (3×10^5 total cells/flask) were replated into 75 cm^2 flask in 15 mL MSC culture medium. Also, 75 cm^2 flasks were placed in the incubator; these cells are referred to as passage 1.

6.2.6 Cryopreservation of WT apBM-MSCs and Gal KO apBM-MSCs

Even we can conduct research without cryopreservation, for our convenience, we cryopreserved created MSCs.

We washed the cells with 8 mL PBS (−) and added 2.4 mL of 0.25% trypsin per 75 cm^2 flask. The cells were kept in the incubator for several minutes at 37 °C. Once the cells were detached, the trypsin was neutralized with 12.6 mL of MSC culture medium per 75 cm^2 flask. The cell suspensions were collected into a 50 mL tube. The cell suspensions were centrifuged for 5 min at 500 × *g* at RT. The isolated WT apBM-MSCs and Gal KO apBM-MSCs were resuspended at 3×10^6 cells/mL to 6×10^6 cells/mL with Cellstor®-S (lactated Ringer's solution with 3% trehalose and 5% dextran 40) containing 10% DMSO. One milliliter of isolated WT apBM-MSCs and Gal KO apBM-MSCs was placed in each cryovial. The cryovials in a BICELL (Nihon Freezer Co., Ltd., Tokyo, Japan) were put in −80°C freeze for 24 h and eventually transferred to liquid nitrogen tank for long-term storage.

6.2.7 Thawing and culture of WT apBM-MSCs and Gal KO apBM-MSCs

The WT apBM-MSCs and Gal KO apBM-MSCs in a cryovial was quickly thawed in a 37 °C water bath. Ten milliliters of MSC culture medium was gently added to the thawed cell suspension, and centrifuged for 5 min at 500 × *g* at RT. The supernatant was removed and 10 mL of MSC culture medium was gently added to the pellet. The pellet was gently resuspended in MSC culture medium by pipetting up and down. The numbers of total and dead cells were counted. The cell suspensions (3×10^5 total cells/flask) were seeded into 75 cm^2 flask in 15 mL MSC culture medium. The 75 cm^2 flask was placed in the CO_2 incubator and incubated at 37 °C, 5% CO_2 and 90% humidity. The medium was refreshed once every 3 days. We washed the cells with 8 mL PBS (−) and added 2.4 mL of 0.25% trypsin per 75 cm^2 flask. The cells were kept in the incubator for several minutes at 37 °C. Once the cells were detached, the trypsin was neutralized with 12.6 mL of MSC culture medium per 75 cm^2 flask. The cell suspensions were collected into a 50 mL tube. The cell suspensions were centrifuged for 5 min at 500 × *g* at RT, and the supernatant was aspirated. The cells were suspended in MSC culture medium and used for each experiment.

6.2.8 Cell viability

Cell viability was determined manually with a plastic cell counting plate (OneCell Counter, Fine Plus International Ltd., Kyoto, Japan) under a microscope by Trypan blue staining. Cell viability was calculated according to formulas below.

Cell viability [%] = (Total cell count - dead cell count) / (Total cell count) × 100.

6.2.9 Cell proliferation assay

To plot the growth curve, passage-four cells were plated at a density of 5,000 cells/cm^2 (1.25×10^5 cells/flask) in 25 cm^2 flask. The MSC culture media was changed every 3 days. The same flasks were trypsinized, and the number of total cells was counted at 1, 2, 4, and 8 days. The growth curve was then plotted using the cell counting data. The doubling time (DT) was calculated using the following formula: doubling time (h) = $[\{(T - T_0)(\log_2)\}/(\log N - \log N_0)]$, where T is the time (h) and N is the cell count.

6.2.10 Analysis of cell size

Analysis of cell size was performed at the end of passage using a NuceloCounter NC-200 (M&S TechnoSystems, Inc.).

6.2.11 Quantification of cell surface marker

To examine the cell surface immunophenotypes and forward scatter, 1×10^7 cells/mL (20–100 μL) in Stain Buffer with FBS (BD Biosciences, San Jose, CA, USA) or 2.5%FBS/PBS/1 mM $CaCl_2$ were incubated for 45–120 min on ice with Isolectin GS-IB4 From Griffonia simplicifolia, Alexa Fluor™ 488 Conjugate (Thermo Fisher Scientific, Inc., MA, USA), Alexa Fluor 647-labeled antibody against pig CD29 (BD Biosciences, Clone NaM160-1A3), Purified mouse against pig SLA-DR(BD Biosciences; Clone 1053H2-18) and FITC-labeled against mouse IgG2a (BD Bioscience; Clone R19-15), phycoerythrin (PE)-labeled antibodies against rat CD31

(BD Biosciences; Clone TLD-3A12), against mouse CD44 (GeneTex, Inc., Irvine, CA, USA; Clone MEM-263), against human CD90 (BD Biosciences; Clone 5E10) and Alexa Fluor 488-labeled antibody against human CD34 (Abcam, Cambridge, England; Clone EP373Y) crossing to pig, or respective isotype controls (BD Biosciences). After washing, the labeled cells were analyzed using a Gallios Flow Cytometer (Beckman Coulter, Indianapolis, IN, USA).

6.2.12 Chondrogenic, osteogenic, and adipogenic differentiation

We performed the induction of the chondrogenic, osteogenic, and adipogenic differentiation of WT apBM-MSCs and Gal KO apBM-MSCs. Induction of chondrogenic differentiation was performed according to the procedure manual of Poietics human mesenchymal stem cells—Chondrogenic assay procedure (Lonza Walkersville, Inc.), and evaluated by alcian blue stain. Induction of osteogenic differentiation was performed according to the procedure manual of Poietics human mesenchymal stem cells —Osteogenic assay procedure (Lonza Walkersville, Inc.), and evaluated by Alkaline Phosphatase Staining kit (AK20, Cosmo Bio Co., Ltd.). Induction of adipogenic differentiation was performed according to Poietics human mesenchymal stem cells—Adipogenic assay procedure (Lonza Walkersville, Inc.), and evaluated by Oil Red staining.

6.2.13 Colony-forming unit (CFU) assay

Cells were plated at a density of 315 cells in 21 cm^2 culture dish (30 cells/cm^2). The MSC culture media was changed on day 3. After 6 days' culture, adherent cells were

washed twice with 4 mL PBS and fixed with 4 mL ice-cold methanol for 15 min at 4 °C. To visualize colonies, cells were stained with 4 mL Giemsa diluted 1:19 with phosphate buffer for 30 min at RT and washed twice with H_2O. The number of colonies that contained more than 50 cells were counted. The colony-forming efficiency of cells was calculated by dividing the number of colonies per dish by the number of cells (315) seeded per dish.

6.2.14 mRNA expression level after cytokine stimulation

The cell suspensions (2×10^5 total cells/plate) seeded into six-well plate in a 2 mL MSC culture medium. The six-well plate was placed in the CO_2 incubator and incubated at 37 °C, 5% CO_2, and 90% humidity. After 24 h, the MSC culture medium was changed in MSC culture medium containing without or with both 5 ng/mL recombinant human interferon-gamma (R&D Systems, Inc., Minneapolis, MN, USA) and 5 ng/mL recombinant human transforming growth factor-alpha (R&D Systems, Inc.). After 24 h, total RNA was extracted from the apBM-MSC using the QIAshredderTM and RNeasy Mini Kit (Qiagen, Hilden, Germany) following the manufacturer's instructions. Total RNA was measured RNA amount by NanoDrop 200c (Thermo Fisher Scientific Inc.).

6.2.15 Oligonucleotides

The pairs of primers and the TaqMan probes (Table 6.1) for the porcine target mRNAs were synthesized by Applied Biosystems, Thermo Fisher Scientific Inc. The GenBank accession numbers are also shown in Table 6.1. Each primer and/or probe homology was searched by an NCBI BLAST search to ensure that it was specific for the target

mRNA transcript. The TaqMan probes contained 6-carboxyfluorescein at the 5′ end and 6-carboxytetramethylrhodamine at the 3′ end and were designed to hybridize to a sequence located between the PCR primers.

Table 6.1. Primers and probes used for RT-PCR analysis of porcine target mRNA

mRNA (GenBank accession number	Sequence
HPRT1 (NM_001032376)	
Forward primer	5′ -AGTGATGACGAACCAGGTTATGAC-3′
Reverse primer	5′ -CTCTTTCATCACATCTCGAGCAA-3′
Probe	5′ -CATGGACTAATTATGGACAGGACTGAACGG-3′
VEGFA (NM_214084)	
Forward primer	5′ -TGTGCCCACTGAGGAGTTCA-3′
Reverse primer	5′ -TCCTATGTGCTGGCCTTGGT-3′
Probe	5′ -CATCGCCATGCAGATTATGCGGATC-3′
IGF1 (NM_214256)	
Forward primer	5′ -CTGGTGGACGCTCTTCAGTTC-3′
Reverse primer	5′ -GAAGCAGCACTCATCCACGAT-3′
Probe	5′ -ATTTCAACAAGCCCACAGGGTACGGC-3′
ADM (NM_214107)	
Forward primer	5′ -TCCCGTAGCCCTCATGTACCT-3′
Reverse primer	5′ -TTCCACGACTTAGAGCCCACTTA-3′
Probe	5′ -TGGCGGCAGAGTTCCGAAAGAAATG-3′
IDO1 (NM_001246240)	
Forward primer	5′ -GCAGCGCCTGGCACAT-3′
Reverse primer	5′ -GGCAGTCCAAGCTTCTCAGAGA-3′
Probe	5′ -ATGAAGATATCCGCAAGGTCCTGCCA-3′
PTGES (NM_001038631)	
Forward primer	5′ -CAAGATGTACGTAGTGGCCATCA-3′
Reverse primer	5′ -CTCCGTGTCTCTGAGCATCCT-3′
Probe	5′ -TTCGGAAGAAGGCTTTTGCCAACCC-3′
PTGS2 (NM_214321)	
Forward primer	5′ -GGCATCACCCAATTTGTTGAAT-3′
Reverse primer	5′ -TCTGGTCGATTGAGGCCTTT-3′
Probe	5′ -AGGCAAATTGCTGGCAGGGTTGCT-3′

HPRT1, hypoxanthine phosphoribosyltransferase 1 (housekeeping gene); VEGFA, vascular endothelial growth factor A; IGF1, insulin-like growth factor 1; ADM, adrenomedullin; IDO1, indoleamine 2,3-dioxygenase 1; PTGES, prostaglandin E synthase; PTGS2, prostaglandin-endoperoxide synthase 2.

6.2.16 TaqMan RT-PCR conditions

Total RNA was diluted to about 20 μg/mL with 50 μg/mL yeast tRNA (Thermo Fisher Scientific Inc.). RT-PCR assay was performed in 20 μL of TaqMan RNA-to-CT 1-Step Kit (Applied Biosystems, Thermo Fisher Scientific Inc.) containing 300 nM forward primer, 900 nM reverse primer, 200 nM TaqMan probe, and 60 ng of total RNA. One-step RT-PCR assay was performed using the Applied Biosystems 7500 Fast Real-Time PCR System with the following profile: 1 cycle at 48 °C for 15 min, 1 cycle at 95 °C for 10 min, and 40 cycles at 95 °C for 15 s and 60 °C for 1 min.

6.2.17 Analysis and statistics

The threshold cycle (*Ct*) was calculated by the instrument's software (7500 Fast System version 2.3). Relative expression of each mRNA was calculated using the Δ*Ct* method (where Δ*Ct* is the value obtained by subtracting the *Ct* value of HPRT1 mRNA from the *Ct* value of the target mRNA). Specifically, the amount of target mRNA relative to HPRT1 mRNA is expressed as $2^{-(\Delta Ct)}$. Data are expressed as the ratio of target mRNA to HPRT1 mRNA.

The mean ± standard deviation of each group was determined. Data were analyzed with SAS 9.4 (SAS Institute Inc., Cary, NC, USA). Statistical analysis was performed using Student's *t*-test, and significance level less than 5% was judged as significant.

6.3 Results

6.3.1 Gal antigen of WT apBM-MSCs and Gal KO apBM-MSCs

WT apBM-MSCs are positive for the Gal antigen. On the other hand, Gal KO apBM-MSCs are negative for the Gal antigen (Figure 6.1).

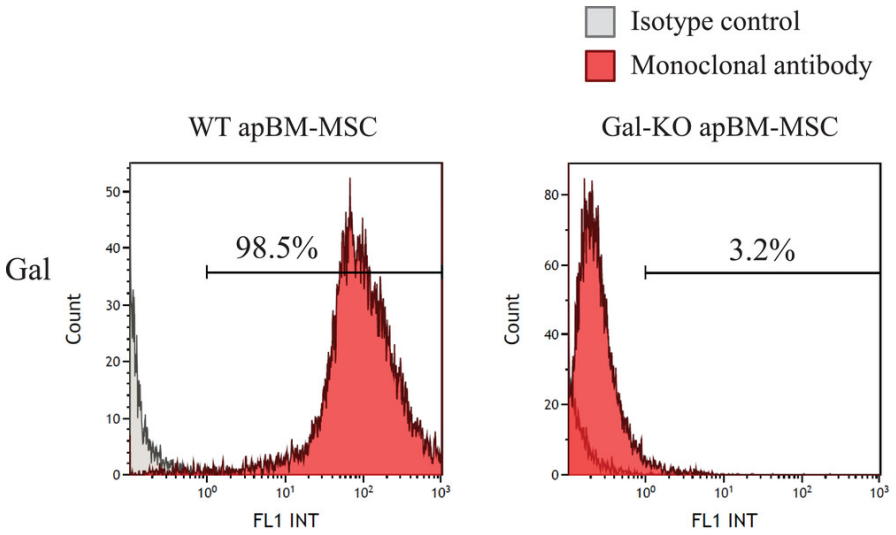

Figure 6.1. Gal antigen on the cell surface of WT apBM-MSCs and Gal KO apBM-MSCs as analyzed by flow cytometry. WT apBM-MSCs and Gal KO apBM-MSCs used passage-3 cells

6.3.2 Growth kinetics and cell size of WT apBM-MSCs and Gal KO apBM-MSCs

At the four passages, the WT apBM-MSCs and Gal KO apBM-MSCs were seeded at 5,000 cells/cm^2 (1.25 × 10^5 cells/flask) in a 25 cm^2 flask, and both cells were about 80% confluence on day 4 and 100% confluence on day 6 (Figure 6.2).

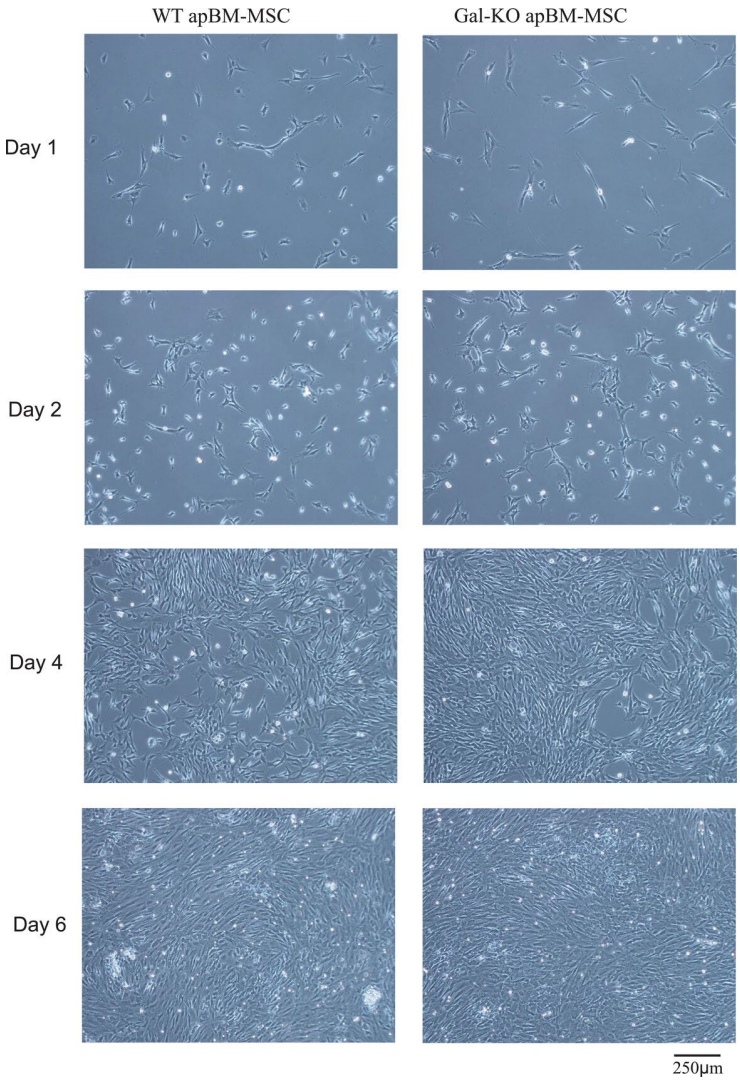

Figure 6.2. Cell growth of WT apBM-MSCs and Gal KO apBM-MSCs. Passage-4 cells were plated at a density of 5,000 cells/cm^2 (1.25 × 10^5 cells/flask) in 25 cm^2 flask. The microscopic analysis showed the appearances of cell growth were similar between the WT apBM-MSCs and Gal KO apBM-MSCs

The calibrated growth curve was plotted for WT apBM-MSCs at P4 and Gal KO apBM-MSCs at P4 (Figure 6.3A). DT of WT apBM-MSCs and Gal KO apBM-MSCs were 24.5 ± 0.5 h and 25.2 ± 0.3 h, respectively, which were not significantly different (Figure 6.3B).

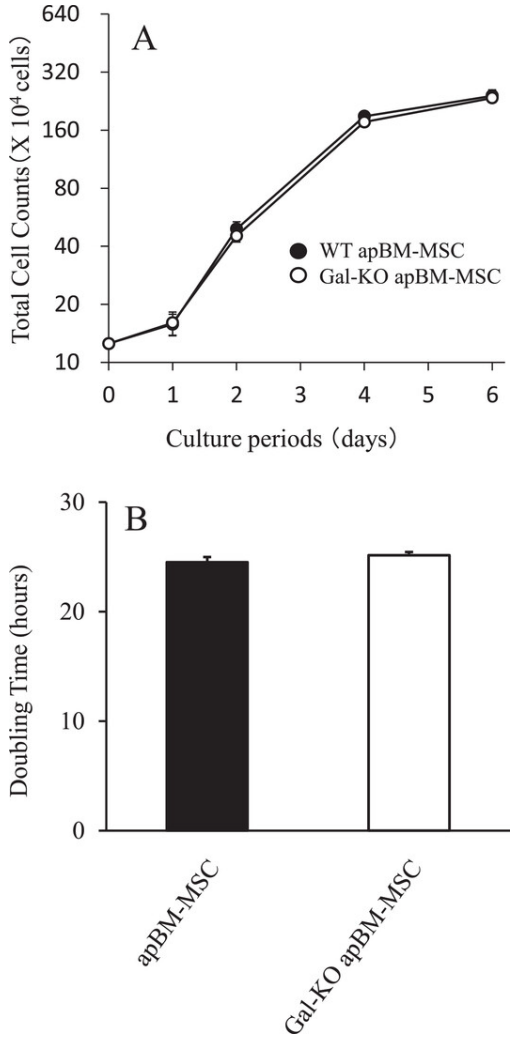

Figure 6.3. Growth curve in WT apBM-MSCs (solid circles) and Gal KO apBM-MSCs (open circles) (A) and DT (B). To plot the growth curve, passage-4 cells were plated at a density of 5,000 cells/cm^2 (1.25 × 10^5 cells/flask) in 25 cm^2 flask. Same flasks were trypsinized, and counted the total number of cells after 1, 2, 4, and 6 days. The growth curve was then plotted using the cell counting data. The DT was calculated from total cell counts of immediately and 96 h after inoculation. Results are shown as mean ± SD (n = 4). There were no significant differences between two groups

The mean diameters of WT apBM-MSCs and Gal KO apBM-MSCs were 14.3 ± 0.5 and 15.1 ± 0.1 μm, respectively. The cell size of Gal KO apBM-MSCs was significantly larger than WT apBM-MSCs ($p < .05$), but the difference was slight (Figure 6.4).

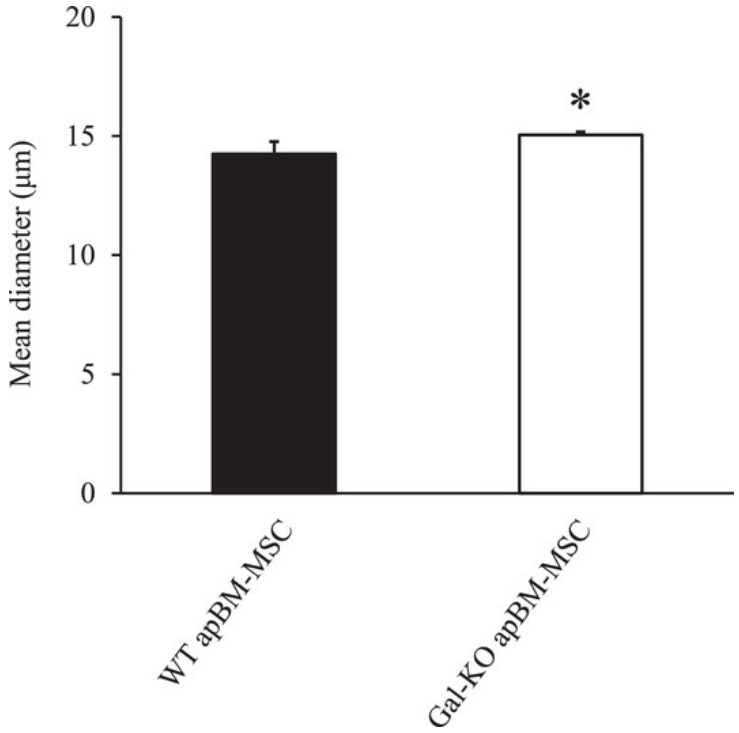

Figure 6.4. Mean diameters of WT apBM-MSCs and Gal KO apBM-MSCs. WT apBM-MSCs and Gal KO apBM-MSCs used passage-4 cells and conducted four experiments. Results of WT apBM-MSCs and Gal KO apBM-MSCs are shown as mean ± SD (n = 4). The diameter of Gal KO apBM-MSCs was significantly larger compared with the diameter of WT apBM-MSCs (Student's *t*-test, $*p < 0.05$)

6.3.3 Immunological surface phenotypes of WT apBM-MSCs and Gal KO apBM-MSCs

Negative surface markers, such as the endothelial marker CD31 and hematopoietic marker SLA-DR (marker of swine corresponding to major histocompatibility antigen HLA-DR of human cells), were little or no detectable in WT apBM-MSCs and Gal KO apBM-MSCs (Figure 6.5A). However, negative surface marker, such as hematopoietic marker CD34, was expressed a little (3.2 and 8.6%) in WT apBM-MSCs and Gal KO apBM-MSCs, respectively (Figure 6.5A). Positive surface markers for MSC, such as CD29, CD44, and CD90, were highly expressed (Figure 6.5B).

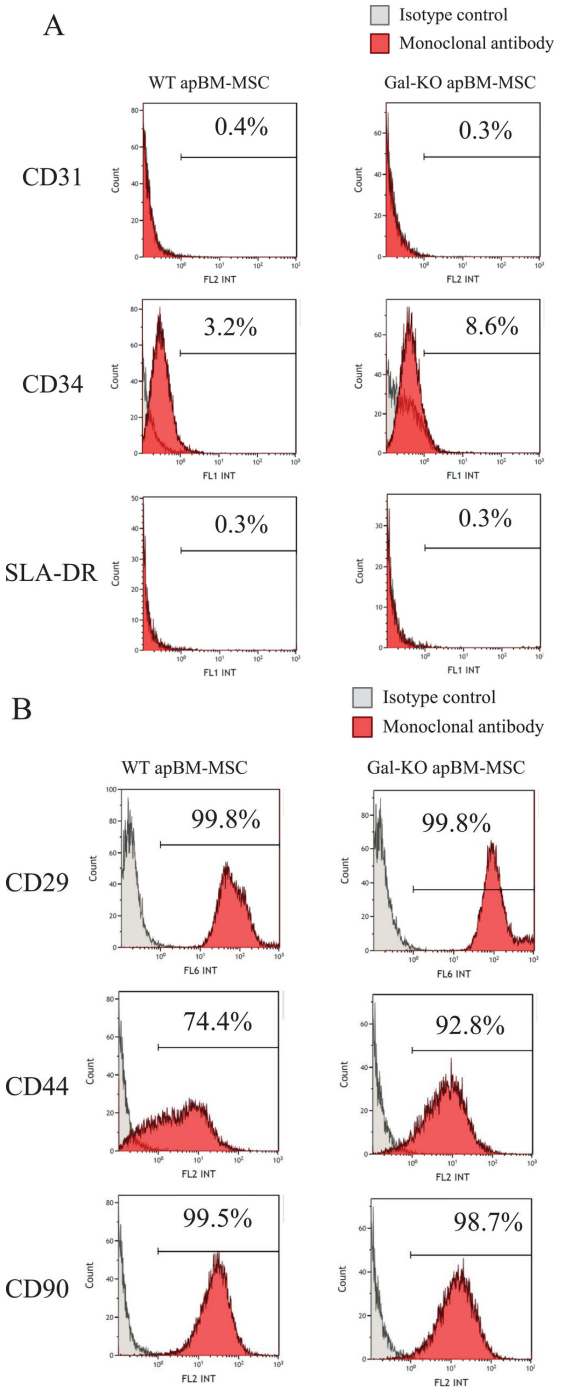

Figure 6.5. Immunophenotypes on the cell surface of WT apBM-MSCs and Gal KO apBM-MSCs as analyzed by flow cytometry. WT apBM-MSCs and Gal KO apBM-MSCs used passage-3 cells. Both WT apBM-MSCs and Gal KO apBM-MSCs are negative for the endothelial marker CD31, and hematopoietic markers SLA-DR. Also, both WT apBM-MSCs and Gal KO apBM-MSCs are a little positive for hematopoietic marker CD34. Both WT apBM-MSCs and Gal KO apBM-MSCs are prominently positive for CD29, CD44, and CD90.

6.3.4 Adipogenic, osteogenic, and chondrogenic differentiation of WT apBM-MSCs and Gal KO apBM-MSCs

Oil Red stain (Figure 6.6A), alkaline phosphatase stain (Figure 6.6B), and alcian blue stain (Figure 66.C) were all positive. Therefore, our WT apBM-MSCs and Gal KO apBM-MSCs could differentiate into three different adipocytes, osteocytes, and chondrocytes.

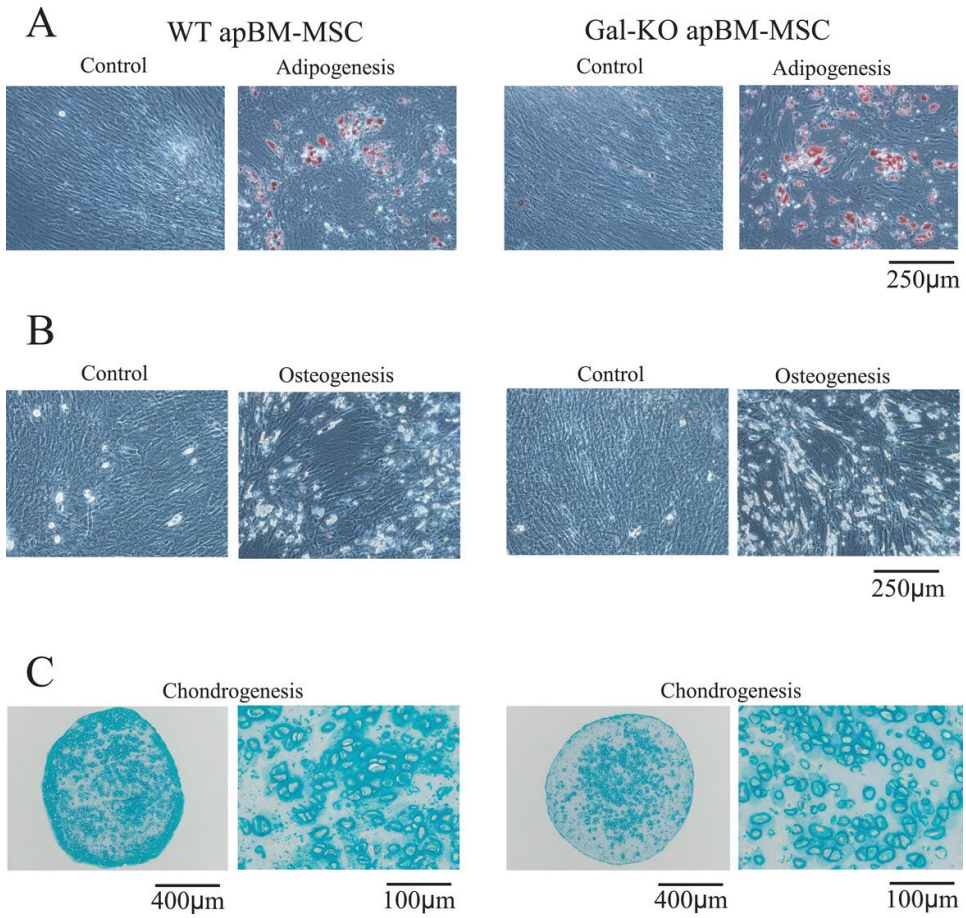

Figure 6.6. Differentiation potential of the WT apBM-MSCs and Gal KO apBM-MSCs. WT apBM-MSCs and Gal KO apBM-MSCs used passage-4 cells. Induction of adipogenic differentiation was evaluated by Oil Red staining (A). Induction of osteogenic differentiation was evaluated by alkaline phosphatase staining (B). Induction of chondrogenic differentiation was evaluated by alcian blue staining (C).

6.3.5 CFS assay of WT apBM-MSCs and Gal KO apBM-MSCs

The colony-forming efficiency of cells of WT apBM-MSCs and Gal KO apBM-MSCs were 44.1 ± 5.9 and 18.3 ± 4.5 μm, respectively, and the colony-forming efficiency of cells of Gal KO apBM-MSCs was significantly lower than WT apBM-MSCs ($p < 0.01$) (Figure 6.7).

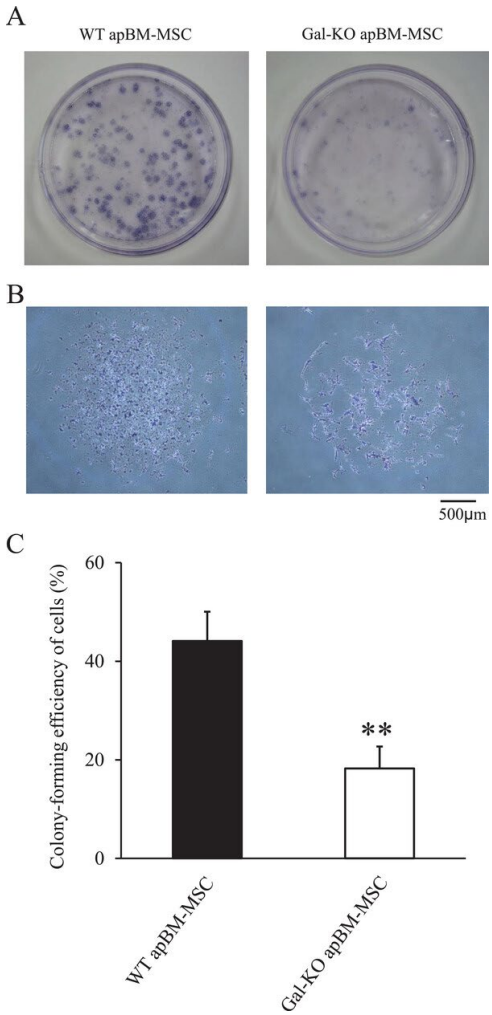

Figure 6.7. CFS assay of WT apBM-MSCs and Gal KO apBM-MSCs. WT apBM-MSCs and Gal KO apBM-MSCs used passage-4 cells and conducted four experiments. Representative images (A) of dish, representative images (B) of colony, and colony-forming efficiency of cells (%) (C). Student's *t*-test (**$p < 0.01$).

6.3.6 mRNA expression level after cytokine stimulation

The mRNA expression levels of vascular growth-related factors (VEGFA, IGF1, and ADM) and immunosuppressive genes (IDO1, PTGES, and PTGS2) were significantly upregulated by cytokine stimulation in both WT apBM-MSCs and Gal KO apBM-MSCs (Figure 6.8).

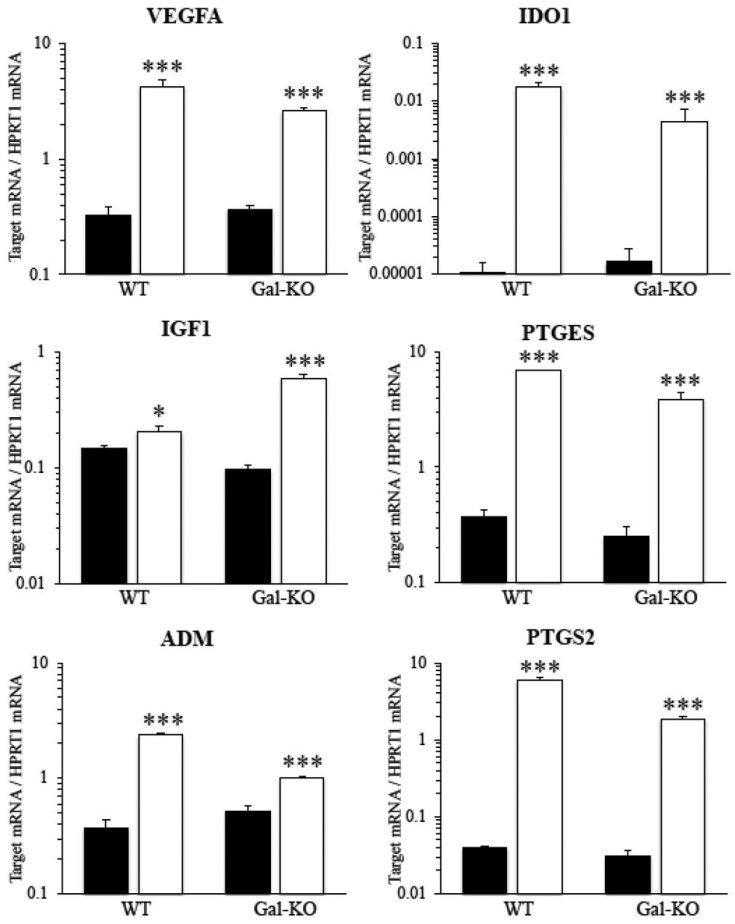

Figure 6.8. mRNA expression of WT apBM-MSCs and Gal KO apBM-MSCs subculture with cytokine stimulation. WT apBM-MSCs and Gal KO apBM-MSCs used passage-3 cells. Data are expressed as the ratio of the target mRNA to HPRT mRNA. The data are presented as the mean ± SD (n = 3). The closed column and open column are without and with cytokine stimulation, respectively. Statistical analysis was performed using Student's *t*-test between subculture without and with cytokine stimulation. *$p < .05$, ***$p < 0.001$.

6.4 Discussion

To overcome the issue of donor limitation of human MSCs, we established the MSCs from the bone marrow of clinical-grade neonatal porcine [Nishimura *et al.* 2019]. Interestingly, the porcine-derived MSC showed rapid growth and small diameter compared to human MSCs [Nishimura *et al.* 2019]. Recently, we demonstrated that the porcine-derived MSCs improved critical ischemic limb disease in rat model more efficiently compared with murine MSCs [Yamada *et al.* 2021]. On the other hand, since porcine MSC is xenogeneic against human, the implanted MSCs could be eliminated by the xenogeneic rejection. Therefore, it is possible to improve the efficacy, if such xenogeneic rejection could be mitigated.

In fact, Li *et al.* have already demonstrated that Gal KO BM-derived porcine MSCs are significantly less immunogenic than WT porcine MSCs, and downregulate the human T-cell response to pig antigens as efficiently as human MSCs do [Li *et al.* 2014]. This encouraged us to investigate whether Gal KO porcine BM-derived MSCs are more efficiently improving the critical ischemic limb disease with our developed method using clinical-grade pigs [Nishimura *et al.* 2019]. Before conducting the research to examine the efficacy on the critical ischemic limb disease, in this report, we have produced Gal KO apBM-MSCs and characterize them. Especially, we compared angiogenesis and immunosuppression-related genes between WT apBM-MSC and Gal KO apBM-MSCs.

Our created Gal KO apBM-MSCs had no Gal antigen in contract to WT apBM-MSC which showed positive Gal antigen as expected. Gal KO apBM-MSCs, like WT apBM-MSCs, detected little or no negative surface markers of MSCs. Of note, we found 10% expression of CD34 which is a hematopoietic marker. However, it is

published that the expression of CD34 in MSCs can happen and it depends on the conditions [Lin *et al.* 2012]. We have also confirmed that the expression of CD34 in commercial human MSCs is about 10% [Fujita *et al.* 2021]. Therefore we consider approximately 10% expression of hematopoietic marker does not deny the identity of MSCs. While Gal KO apBM-MSCs detected positive surface markers of MSCs.

Furthermore, Gal KO apBM-MSCs were able to differentiate into adipocytes, osteocytes, and chondrocytes as well as WT apBM-MSCs. There was also no difference in DT between Gal KO apBM-MSCs and WT apBM-MSCs. In fact, the DT of human bone marrow-derived MSC was approximately 60 h [Nishimura *et al.* 2019]. Therefore, both the DT of WT apBM-MSCs and Gal KO apBM-MSCs were less than half of the hBM-MSCs.

However, the colony-forming efficiency of Gal KO apBM-MSCs was about half that of WT apBM-MSCs, and the density of cells in the colony was also smaller when observed under the microscope. The colony-forming efficiency of WT apBM-MSCs in this report is 44.1%, and the report by Antebi *et al.* was also shown that the colony-forming efficiency of MSCs prepared from the bone marrow of Yorkshire female cross-bred swine was about 40% [Antebi *et al.* 2018]. On the other hand, the colony-forming efficiency of Gal KO apBM-MSCs in this report is 18.3%. This value was close to the colony-forming efficiency of human bone marrow- and pancreas-derived MSCs (about 10%) reported by Thirlwell *et al.*[Thirlwell *et al.* 2020.] and the colony-forming efficiency of human adipose tissue-derived MSCs (about 20%) reported by Fujita *et al.* [Fujita *et al.* 2020.] Gal antigen is negative in human [Galili *et al.* 2013], therefore, Gal antigen may have some role in the process of cell adhesion and colony formation. Considering proliferation rates are similar between the WT apBM-MSCs and Gal KO apBM-MSCs (Figure 6.3), we speculate that low colony-forming ability is associated

with low expression of adhesion molecule in Gal KO apBM-MSCs. We plan to assess the adhesion molecule to examine our speculation.

To assess the efficacy of Gal KO apBM-MSCs, we measured the expression levels of genes related to angiogenesis (VEGFA, IGF1, and ADM) and immunosuppression-related genes (IDO1, PTGES, and PTGS2) stimulated by cytokine. All six genes were upregulated by cytokine stimulation and the levels of upregulation are similar between the Gal KO apBM-MSCs and WT apBM-MSC. At least, we have confirmed Gal KO apBM-MSCs have similar effects to WT apBM-MSC related to angiogenesis and immunosuppression-related genes, even Gal KO apBM-MSCs have significant lower efficacy of colony forming.

In this study, to address whether we can establish and characterize the MSC from Gal KO pigs, we used already established adult Gal KO pigs [Tanihara *et al.* 2020]. Now, we confirmed it is possible to create and characterize the MSC from Gal KO pigs, we plan to create Gal KO neonatal porcine BM-MSCs toward a clinical application.

6.5 Conclusions

We have developed and characterized Gal KO apBM-MSCs. Gal KO apBM-MSCs have maintained the majority of MSC characteristics including angiogenesis and immunosuppression-related gene upregulation by cytokine stimulation. With this finding, we plan to conduct next experiments using neonatal porcine towards clinical trial.

7. Overall conclusion

The results of this study suggested a method to minimize the risk of embolism during intravascular administration of MSCs and the possibility of using pigs as a donor source to ensure a stable supply of MSCs, both of which are necessary for further development of MSC-based therapies.

In cell therapy using MSCs, cells are administered to patients in anticipation of the ability of MSCs to differentiate, secrete cytokines, and immunoregulate. Naturally, the administered MSCs must show high viability. As shown in Chapters 3 and 4 of this study, lactated Ringer's solution with 3% trehalose and 5% dextran 40 (LR-3T-5D: Cellstor S) was able to maintain MSCs from human adipose and human bone marrow at 25 °C and 5 °C without loss of viability for 24 h. The ability to maintain cell viability not only under low-temperature preservation conditions, but also at room temperature, the assumed temperature used for bedside slow cell administration, is very important to ensure the therapeutic efficacy of MSCs. Since the viability of the assessed cells decreased after preservation in lactated Ringer's solution, it can be assumed that the maintained viability is due to the protective effect of trehalose. However, the study also demonstrated that cell aggregation occurs when cells are preserved at 25 °C for 24 h. MSCs are adhesive cells, and one of their characteristics is the ability to adhere to containers during culture [Dominici *et al*. 2006]. The use of low-adhesion test tubes (STEMFULL™) avoids adherence to the container and improves cell recovery after storage. On the other hand, MSCs also adhere to each other and form spheroids when cultured in low-adhesion containers [Cesarz *et al*. 2016]. It is assumed that aggregation occurs because MSCs with high viability adhere to each other due to their inherent self-adherent property. In fact, no aggregation was observed when the hBM-MSCs and

hADSCs, whose viability decreased during preservation, were preserved in lactated Ringer's solution. No cell aggregation occurred after 24 h of storage under low temperature conditions, which is assumed to be a result of suppression of cell adhesion-related protein function. Whenever possible, cells should be stored at a low temperature. However, there are occasions when room-temperature storage of cells is necessary, such as slow cell administration at the bedside. Therefore, we also investigated conditions under which aggregation would be suppressed, even during storage at 25 °C.

In Chapter 3, we showed that increasing the heparinization time from 5 to 10 min before cell collection could suppress the aggregation of hBM-MSCs. A number of reports have indicated that trypsin treatment decreases the expression of surface proteins on MSCs [Tsuji *et al*. 2017, Garg *et al.* 2014, Nakao *et al.* 2019]. High concentrations of trypsin were shown to suppress CXCR4 expression in BM-MSCs [Pervin *et al*. 2021]. N-cadherin is required for the aggregation of HEK293T cells after trypsin detachment, and suppressing N-cadherin also suppresses aggregation [Tachibana 2019]. We therefore propose that a trypsin treatment time of 10 min suppresses the function of surface proteins involved in adhesion, including cadherins, thereby also suppressing storage-associated aggregation.

Furthermore, a study of preservation of hADSCs at 25 °C indicated that the higher the Oxygen partial pressure (pO_2) in the preservation solution, the more likely cell aggregation was to occur. The pO_2 in the preservation solution could be reduced by replacing the headspace in the storage container with nitrogen gas, which also reduced the cell aggregation rate. Even without nitrogen gas, pO_2 in the preservation solution could be reduced and cell aggregation could be suppressed by increasing the amount of preservation solution and the cell concentration during cell preservation. We hypothesize that the pO_2 in the solution decreases because the volume of the air layer in

the tube and the gas exchange efficiency from the surface of the solution decrease when the volume of the solution increases. Preserving cells as higher-density suspensions decreases the pO_2, presumably as a result of increased oxygen consumption due to the increased number of cells in the suspension. These are very reasonable and useful techniques because they do not require special equipment or reagents. In the present study, nitrogen gas replacement significantly inhibited cell aggregation by reducing the pO_2 of the preservation solution to 46.6 mmHg after 24 h of storage. The pO_2 in normal adipose tissue is approximately 50 mmHg, and one study suggests that adipose tissue-derived MSCs are inherently hypoxia tolerant; oxygen levels as low as 1% had no effect on survival [Suga *et al*. 2010]. Indeed, in the present study, the viability of hADSCs was not affected even under nitrogen gas replacement conditions, suggesting that hypoxia itself not only inhibits cell aggregation but also poses a low risk to the cells. In studies using cancer cells, hypoxia has been shown to suppress the expression of cell surface proteins such as cadherins [Zhang *et al*. 2015, Duś-Szachniewicz *et al.* 2018]. On the other hand, studies with vascular endothelial cells and human umbilical vein endothelial cells have shown that exposure to reactive oxygen species (ROS) results in altered expression of cell surface proteins and increased adhesion [Patel *et al.* 1991, Sellak *et al.* 1994]. Although which factors mediate the effects of ROS on cell adhesion remain unclear, lowering the pO_2 in the suspension may suppress ROS generation. The conditions that decrease pO_2 in this study may suppress the aggregation of preserved cells by decreasing ROS production and controlling changes in the expression of cell surface proteins.

All of the preservation experiments in this study utilized low-adhesion containers. If non-low-adhesion containers are used to preserve MSCs for 24 h at 25 °C, the cells may adhere to the containers. Adhesion of cells to the container would be unfavorable

for cell therapy because of issues such as insufficient cell retrieval or doses containing lower than the recommended amount of cells. We assume that the aggregation suppression method demonstrated in this study is container-independent and can suppress cell adhesion to non-adhesive containers.

In Chapters 5 and 6, we studied the possibility of using pigs as a stable source of MSCs to expand the therapeutic applications of MSCs. In particular, Chapter 5 investigated the establishment of MSCs from designated pathogen-free clinical-grade pigs to reduce the transmission risk of infectious diseases from pigs, which is one of the issues that must be resolved in xenotransplantation. At the same time, since it is important to be able to cryopreserve the derived tissues for a stable supply of MSCs, we also examined the cryopreservation of the derived tissues. MSCs were established from cryopreserved islets using a more general and simple method of slow freezing and thawing in a warm water bath at 37 °C. Although pig islets have a fragile constitution [Salama *et al.* 2017], we have demonstrated that they can be used to establish MSCs at any time, even after being frozen for more than 4 years. Although islets cryopreserved by the simple slow freezing method would have reduced function as endocrine cells, they could be used without issue as a source for the establishment of MSCs, in light of the freezing tolerance of MSCs [Marquez-Curtis *et al*. 2015]. Islets isolated for human transplantation are also used for basic research if they do not fulfill the transplantation criteria [Kin *et al*. 2011]. As one possibility, it was suggested to utilize pancreatic islets, which were assumed to have poor function, as a source for establishing MSCs. If islets that cannot be transplanted can be used as a source for establishing MSCs for human transplantation, this will expand the effective utilization of islets.

No significant differences were observed in cell proliferation rate and doubling time, cell diameter, and positive and negative markers of MSCs when comparing

clinical-grade and non-clinical-grade islet MSCs. Compared to BM-MSCs, the cell diameter was larger, proliferation speed was slower, and colony-forming efficiency was superior. We believe that this is not due to the characteristics of the clinical grade, but rather to differences in MSC characteristics due to differences in the tissues from which the MSCs were derived, as has been reported in several previous studies [Mutskov *et al*. 2007, Ruetze *et al*. 2014, Cooper *et al*. 2020, Cooper *et al*. 2021, Pomato *et al*. 2021]. The results of this evaluation suggest that there is no difference between MSCs established from cryopreserved islets of clinical-grade pigs and non-clinical-grade pigs, and that the therapeutic effects of MSCs are similar. However, a next step is to more accurately characterize MSCs by evaluating gene expression, cytokine secretion, and immunosuppressive ability, which are directly related to therapeutic efficacy.

Chapter 6 focuses on the suppression of hyperacute rejection, which must be resolved in xenotransplantation. Previously, we created Gal-KO pigs using genome editing technology [Tanihara *et al.* 2020], and used the Gal-KO pigs as a cell source for MSCs. Gal-KO pigs have been shown to have decreased Gal expression in heart, lung, liver, pancreas, and kidney tissues by immunohistological staining. In this study, we confirmed by flow cytometry that Gal expression was also decreased in MSCs established from bone marrow as well as in each tissue. Comparing WT and Gal-KO MSCs, there seems to be no significant difference in proliferation rate, differentiation potential, and expression of MSC positive/negative markers. There was a slight difference in cell diameter, but we believe this was probably just incidental and not due to Gal-KO. No obvious differences in mRNA expression levels of vascular growth-related factors and immunosuppressive genes were observed between the two groups. However, the colony formation efficiency of Gal-KO pig MSCs was about half that of WT pig MSCs, and the cell density in the colony was small when observed under a

microscope. In this study, the colony formation efficiency was 44.1% for WT pig MSCs, which was similar to the colony formation efficiency of about 40% for MSCs prepared from the bone marrow of Yorkshire female crossbred pigs [Antebi *et al*. 2018]. On the other hand, it has been reported that the colony formation efficiency of human bone marrow- and pancreas-derived MSCs is about 10% and that of human adipose tissue-derived MSCs is about 20% [Thirwell *et al*. 2020, Fujita *et al*. 2020]. This value is close to the colony formation efficiency of 18.3% for Gal KO pig MSCs, which is the result of this study. Gal antigen may play some role in the processes of cell adhesion and colony formation, but further studies are needed. It was suggested that when Gal-KO pig MSCs were used for cell therapy, the therapeutic effects of cell differentiation, vascular induction, and immunosuppression may be comparable to those of WT pig-MSCs, with a lower degree of hyperacute rejection compared to WT pig-MSCs.

A next step is to develop genome-edited pigs in a clinical-grade pig breeding environment. We hope to characterize MSCs in pigs with reduced risk of infection and hyperacute rejection, thereby paving the way for the expansion of cell therapy.

This study demonstrated a useful method for suppressing cell aggregation during storage of human MSCs, which is important for intravascular administration. We also showed that cryopreserved islets from clinical-grade neonatal pigs and bone marrow from Gal-KO pigs can be used as sources for establishing MSCs. The results of these studies should be useful for the further development of MSC-based therapies.

8. Acknowledgment

I would like to express my sincere gratitude to Professor Takeshige Otoi of the University of Tokushima for his careful guidance of this research, from the study content to writing of the paper and determining the mindset. I would like to express my gratitude to Professor Taro Mito of the Graduate School of Sciences and Technology for Innovation, Tokushima University and Professor Takefumi Hattori of the graduate school for their guidance as vice-inspectors.

Dr. Masuhiro Nishimura of Otsuka Pharmaceutical Factory, Inc., guided me through the overall process from experimental techniques and data compilation to writing the paper, and Dr. Masako Doi gave me the initial chance and strong encouragement to start this research. Dr. Shinichi Matsumoto, our special advisor, carefully guided us on how to structure and handle the most important steps in submitting a paper for publication. Dr. Akiyoshi Kuroda and Dr. Shigeki Toyoshima, my supervisors at the company, provided me with generous support and advice in the compilation of this study. I would like to thank them from the bottom of my heart.

I would also like to thank Dr. Maki Hirata, Dr. Fuminori Tanihara, Dr. Yasutaka Fujita, Ms. Chikage Shirakawa, Dr. Natsuki Komori, Ms. Naho Iizuka, Mr. Makoto Tanaka, Dr. Osamu Sawamoto, and all others who assisted in this study. I am particularly grateful to Dr. Eiji Kobayashi, who has had the greatest influence on my life by teaching me the joy of research.

Finally, I would like to thank my wife and sons for supporting me outside of my research.

9. Reference

- Adas G, Cukurova Z, Yasar K.K, Yilmaz R, Isiksacan N, Kasapoglu P, *et al.* The systematic effect of mesenchymal stem cell therapy in critical COVID-19 patients: a prospective double controlled trial. *Cell Transplant.* 2021; 30: 9636897211024942.
- Aggarwal S, Pittenger MF. Human mesenchymal stem cells modulate allogeneic immune cell responses. *Blood.* 2005; Feb 15;105(4):1815-22.
- Aikawa E, Fujita R, Asai M, Kaneda Y, Tamai K. Receptor for advanced glycation end products-mediated signaling impairs the maintenance of bone marrow mesenchymal stromal cells in diabetic model mice. *Stem Cells Dev.* 2016; 25(22): 1721–1732.
- Alzebdeh DA, Matthew HW. Metabolic oscillations in co-cultures of hepatocytes and mesenchymal stem cells: effects of seeding arrangement and culture mixing. *J Cell Biochem*. 2017; 118(9): 3003–3015.
- Antebi B, Walker KP 3rd, Mohammadipoor A, Rodriguez LA, Montgomery RK, Batchinsky AI, *et al.* The effect of acute respiratory distress syndrome on bone marrow-derived mesenchymal stem cells. *Stem Cell Res Ther*. 2018; 9(1): 251.
- Berry JD, Cudkowicz ME, Windebank AJ, Staff NP, Owegi M, Nicholson K, *et al.* NurOwn, phase 2, randomized, clinical trial in patients with ALS: safety, clinical, and biomarker results. *Neurology*. 2019; 93(24): e2294–e2305.
- Cai Y, Li J, Jia C, He Y, Deng C. Therapeutic applications of adipose cell-free derivatives: a review. *Stem Cell Res Ther*. 2020; Jul 22; 11(1): 312.
- Cesarz Z, Tamama K. Spheroid Culture of Mesenchymal Stem Cells. *Stem Cells Int.* 2016; 2016:9176357.
- Cooper TT, Sherman SE, Bell GI, Dayarathna T, McRae DM, Ma J, *et al.* Ultrafiltration and injection of islet regenerative stimuli secreted by pancreatic mesenchymal stromal cells. *Stem Cells Dev*. 2021; 30(5): 247–264.
- Cooper TT, Sherman SE, Bell GI, Ma J, Kuljanin M, Jose SE, *et al.* Characterization of a Vimentin^{high}/Nestin^{high} proteome and tissue regenerative secretome generated by human pancreas-derived mesenchymal stromal cells. *Stem Cells*. 2020; 38(5): 666–682.
- Cuesta-Gomez N, Graham GJ, Campbell JDM. Chemokines and their receptors: predictors of the therapeutic potential of mesenchymal stromal cells. *J Transl Med*. 2021; 19(1): 156.

- Davani B, Ikonomou L, Raaka BM, Geras-Raaka E, Morton RA, Marcus-Samuels B, *et al.* Human islet-derived precursor cells are mesenchymal stromal cells that differentiate and mature to hormone-expressing cells in vivo. *Stem Cells*. 2007; 25(12): 3215–3222.
- Dave SD, Patel CN, Vanikar AV, Trivedi HL. In vitro differentiation of neural cells from human adipose tissue derived stromal cells. *Neurol India*. 2018; May-Jun;66(3):716-721.
- Dilogo I.H, Aditianingsih D, Sugiarto A, Burhan E, Damayanti T, Sitompul P.A, *et al.* Umbilical cord mesenchymal stromal cells as critical COVID-19 adjuvant therapy: A randomized controlled trial. *Stem Cells Transl Med.* 2021;10(9):1279–1287.
- Dominici M, Le Blanc K, Mueller I, Slaper-Cortenbach I, Marini F, Krause D, *et al*. Minimal criteria for defining multipotent mesenchymal stromal cells. The International Society for Cellular Therapy position statement. *Cytotherapy.* 2006;8(4):315-7.
- Duś-Szachniewicz K, Drobczyński S, Ziółkowski P, Kołodziej P, Walaszek K.M, Korzeniewska A.K, *et al.* Physiological hypoxia (physioxia) impairs the early adhesion of single lymphoma cell to marrow stromal cell and extracellular matrix. *Optical Tweezers Study. Int J Mol Sci.* 2018;19(7):1880.
- Fishman JA. Infectious disease risks in xenotransplantation. *Am J Transplant*. 2018; Aug;18(8):1857-1864.
- Fu X, Liu G, Halim A, Ju Y, Luo Q, Song AG. Mesenchymal Stem Cell Migration and Tissue Repair. *Cells*. 2019; Jul 28;8(8):784.
- Fujimoto A, Suzuki R, Orihara K, Iida M, Yamashita T, Nagafuji K, *et al.* Health-related quality of life in peripheral blood stem cell donors and bone marrow donors: a prospective study in Japan. *Int J Hematol*. 2020; 111(6): 840–850.
- Fujita Y, Nishimura M, Komori N.W, Wada T, Shirakawa C, Takenawa T, *et al.* A pair of cell preservation solutions for therapy with human adipose tissue-derived mesenchymal stromal cells. *Regen Ther.* 2020;14:95–102.
- Fujita Y, Nishimura M, Komori N, Sawamoto O, Kaneda S. Protein-free solution containing trehalose and dextran 40 for cryopreservation of human adipose tissue-derived mesenchymal stromal cells. *Cryobiology*. 2021; 100: 46-57.
- Galili U. α1,3 Galactosyltransferase knockout pigs produce the natural anti-Gal antibody and simulate the evolutionary appearance of this antibody in primates. *Xenotransplantation*. 2013; 20: 267-276.
- Garg A, Houlihan DD, Aldridge V, Suresh S, Li KK, King AL, *et al*. Non-enzymatic dissociation of human mesenchymal stromal cells improves chemokine-

dependent migration and maintains immunosuppressive function. *Cytotherapy.* 2014; 16(4):545–559.

- Gibbons GW. Grafix®, a cryopreserved placental membrane, for the treatment of chronic/stalled wounds. *Adv Wound Care (New Rochelle)*. 2015; 4(9): 534–544.
- Golchin A, Chatziparasidou A, Ranjbarvan P, Niknam Z, Ardeshirylajimi A. Embryonic Stem Cells in Clinical Trials: Current Overview of Developments and Challenges. *Adv Exp Med Biol*. 2021;1312:19-37.
- Griffith BP, Goerlich CE, Singh AK, Rothblatt M, Lau CL, Shah A, *et al.* Genetically modified porcine-to-human cardiac xenotransplantation. *N Engl J Med*. 2022; 387(1): 35–44.
- Grochowski C, Radzikowska E, Maciejewski R. Neural stem cell therapy-Brief review. *Clin Neurol Neurosurg*. 2018 Oct;173:8-14.
- Gronthos S, Mankani M, Brahim J, Robey PG, Shi S. Postnatal human dental pulp stem cells (DPSCs) in vitro and in vivo. *Proc Natl Acad Sci U S A*. 2000; Dec 5;97(25):13625-30.
- Hillberg AL, Kathirgamanathan K, Lam JB, Law LY, Garkavenko O, Elliott RB. Improving alginate-poly-L-ornithine-alginate capsule biocompatibility through genipin crosslinking. *J Biomed Mater Res B Appl Biomater*. 2013; 101(2): 258–268.
- Ito T, Kenmochi T, Kurihara K, Aida N. The history of clinical islet transplantation in Japan. *J Clin Med*. 2022; 11(6): 1645.
- Kagiwada H, Yashiki T, Ohshima A, Tadokoro M, Nagaya N, Ohgushi H. Human mesenchymal stem cells as a stable source of VEGF-producing cells. *J Tissue Eng Regen Med*. 2008 Jun;2(4):184-9.
- Kaoutzanis C, Gupta V, Winocour J, Layliev J, Ramirez R, Grotting JC, *et al.* Cosmetic liposuction: preoperative risk factors, major complication rates, and safety of combined procedures. *Aesthet Surg J*. 2017; 37(6): 680–694.
- Keshtkar S, Kaviani M, Sarvestani FS, Ghahremani MH, Aghdaei MH, Al-Abdullah IH, *et al.* Exosomes derived from human mesenchymal stem cells preserve mouse islet survival and insulin secretion function. *EXCLI J*. 2020; 19: 1064–1080.
- Kholodenko I.V, Yarygin K.N. Cellular mechanisms of liver regeneration and cell-based therapies of liver diseases. *Biomed Res Int.* 2017;2017: :8910821.
- Kikuchi T, Nishimura M, Hirata M, Tanihara F, Komori N, Tanaka M, *et al.* Development and characterization of Gal KO porcine bone marrow-derived mesenchymal stem cells. *Xenotransplantation*. 2021; 8(6):e12717.
- Kin T, O'Gorman D, Schroeder A, Onderka C, Richer B, Rosichuk S, *et al*. Human

islet distribution program for basic research at a single center. *Transplant Proc*. 2011; Nov;43(9):3195-7.

- Kojayan GG, Alexander M, Imagawa DK, Lakey JRT. Systematic review of islet cryopreservation. *Islets*. 2018; 10(1): 40–49.
- Konishi A, Sakushima K, Isobe S, Sato D. First approval of regenerative medical products under the PMD act in Japan. *Cell Stem Cell*. 2016; 18(4): 434–435.
- Laurenti E, Göttgens B. From haematopoietic stem cells to complex differentiation landscapes. *Nature.* 2018; Jan 24;553(7689):418-426.
- Lechanteur C, Briquet A, Giet O, Delloye O, Baudoux E, Beguin Y. Clinical-scale expansion of mesenchymal stromal cells: a large banking experience. *J Transl Med*. 2016; 14(1): 145.
- Li J, Ezzelarab M, Ayares D, Cooper DK. The potential role of genetically—modified pig mesenchymal stromal cells in xenotransplantation. *Stem Cell Rev*. 2014; 10(1): 79-85.
- Lin CS, Ning H, Lin G, Lue TF. Is CD34 truly a negative marker for mesenchymal stromal cells? *Cytotherapy*. 2012; 14(10): 1159-1163.
- Lin Q, Le QA, Takebayashi K, Hirata M, Tanihara F, Sawamoto O, *et al*. Short-term preservation of porcine zygotes at ambient temperature using a chemically defined medium. *Anim Sci J*. 2022; Jan-Dec;93(1):e13711. - a
- Lin Q, Le QA, Takebayashi K, Hirata M, Tanihara F, Thongkittidilok C, *et al.* Viability and developmental potential of porcine blastocysts preserved for short term in a chemically defined medium at ambient temperature. *Reprod Domest Anim*. 2022; 57(5):556–563. -b
- Linh NT, Paul K, Kim B, Lee BT. Augmenting in vitro osteogenesis of a glycine-arginine-glycine-aspartic-conjugated oxidized alginate-gelatin-biphasic calcium phosphate hydrogel composite and in vivo bone biogenesis through stem cell delivery. *J Biomater Appl*. 2016; 31(5): 661–673.
- Liu J, Ding Y, Liu Z, Liang X. Senescence in Mesenchymal Stem Cells: Functional Alterations, Molecular Mechanisms, and Rejuvenation Strategies. *Front Cell Dev Biol*. 2020; May 5;8:258.
- Makowka L, Wu GD, Hoffman A, Podesta L, Sher L, Tuso PJ, *et al.* Immunohistopathologic lesions associated with the rejection of a pig-to-human liver xenograft. *Transplant Proc*. 1994; Jun;26(3):1074-5.
- Marquez-Curtis LA, Dai XQ, Hang Y, Lam JY, Lyon J, Manning Fox JE, *et al.* Cryopreservation and post-thaw characterization of dissociated human islet cells. *PLoS One*. 2022; 17(1):e0263005.

- Marquez-Curtis LA, Janowska-Wieczorek A, McGann LE, Elliott JA. Mesenchymal stromal cells derived from various tissues: biological, clinical and cryopreservation aspects. *Cryobiology*. 2015; 71(2): 181–197.
- Matsumoto S, Abalovich A, Wechsler C, Wynyard S, Elliott RB. Clinical benefit of islet xenotransplantation for the treatment of type 1 diabetes. *EBioMedicine*. 2016; 12: 255–262.
- Matsumoto S, Qualley SA, Goel S, Hagman DK, Sweet IR, Poitout V, *et al.* Effect of the two-layer (University of Wisconsin solution-perfluorochemical plus O2) method of pancreas preservation on human islet isolation, as assessed by the Edmonton Isolation Protocol. *Transplantation*. 2002; 74(10): 1414–1419.
- Matsumoto S, Tan P, Baker J, Durbin K, Tomiya M, Azuma K, *et al.* Clinical porcine islet xenotransplantation under comprehensive regulation. *Transplant Proc*. 2014; 46(6): 1992–1995.
- McLaren A.J, Friend P.J. Trends in organ preservation. *Transpl Int.* 2003;16(10):701–708.
- Moll G, Ankrum JA, Kamhieh-Milz J, Bieback K, Ringdén O, Volk HD, *et al.* Intravascular mesenchymal stromal/stem cell therapy product diversification: time for new clinical guidelines. *Trends Mol Med*. 2019; 25(2): 149–163.
- Montgomery RA, Stern JM, Lonze BE, Tatapudi VS, Mangiola M, Wu M, *et al.* Results of two cases of pig-to-human kidney xenotransplantation. *N Engl J Med*. 2022; 386(20): 1889–1898.
- Munir H, McGettrick H.M. Mesenchymal stem cell therapy for autoimmune disease: risks and rewards. *Stem Cells Dev.* 2015;24(18):2091–2100.
- Murata M, Terakura S, Wake A, Miyao K, Ikegame K, Uchida N, *et al.* Off-the-shelf bone marrow-derived mesenchymal stem cell treatment for acute graft-versus-host disease: real-world evidence. *Bone Marrow Transplant.* 2021;56(10):2355–2366.
- Mutskov V, Raaka BM, Felsenfeld G, Gershengorn MC. The human insulin gene displays transcriptionally active epigenetic marks in islet-derived mesenchymal precursor cells in the absence of insulin expression. *Stem Cells*. 2007; 25(12): 3223–3233.
- Nakao M, Kim K, Nagase K, Grainger DW, Kanazawa H, Okano T. Phenotypic traits of mesenchymal stem cell sheets fabricated by temperature-responsive cell culture plate: structural characteristics of MSC sheets. *Stem Cell Res Ther*. 2019; 10(1):353.
- Nishimura M, Nguyen L, Watanabe N, Fujita Y, Sawamoto O, Matsumoto S. Development and characterization of novel clinical grade neonatal porcine bone

marrow-derived mesenchymal stem cells. *Xenotransplantation*. 2019; 26(3):e12501.

- Nishimura M, Iizuka N, Fujita Y, Sawamoto O, Matsumoto S. Effects of encapsulated porcine islets on glucose and C-peptide concentrations in diabetic nude mice 6 months after intraperitoneal transplantation. *Xenotransplantation*. 2017; 24(4):e12313.
- Oh JY, Kim MK, Shin MS, Lee HJ, Ko JH, Wee WR, *et al*. The anti-inflammatory and anti-angiogenic role of mesenchymal stem cells in corneal wound healing following chemical injury. *Stem Cells.* 2008 Apr;26(4):1047-55.
- Patel K.D, Zimmerman G.A, Prescott S.M, McEver R.P, McIntyre T.M. Oxygen radicals induce human endothelial cells to express GMP-140 and bind neutrophils. *J Cell Biol.* 1991;112(4):749–759.
- Pervin B, Aydın G, Visser T, Uçkan-Çetinkaya D, Aerts-Kaya FSF. CXCR4 expression by mesenchymal stromal cells is lost after use of enzymatic dissociation agents, but preserved by use of non-enzymatic methods. *Int J Hematol*. 2021; 113(1):5–9.
- Pomatto M, Gai C, Negro F, Cedrino M, Grange C, Ceccotti E, *et al.* Differential therapeutic effect of extracellular vesicles derived by bone marrow and adipose mesenchymal stem cells on wound healing of diabetic ulcers and correlation to their cargoes. *Int J Mol Sci*. 2021; 22(8): 3851.
- Qu W, Wang Z, Engelberg-Cook E, Yan D, Siddik AB, Bu G, *et al.* Efficacy and safety of MSC Cell therapies for hospitalized patients with COVID-19: a systematic review and meta-analysis. *Stem Cells Transl Med*. 2022; 11(7): 688–703.
- Ricordi C, Goldstein JS, Balamurugan AN, Szot GL, Kin T, Liu C, *et al.* National institutes of health-sponsored clinical islet transplantation consortium phase 3 trial: manufacture of a complex cellular product at eight processing facilities. *Diabetes*. 2016; 65(11): 3418–3428.
- Riordan N.H, Morales I, Fernández G, Allen N, Fearnot N.E, Leckrone M.E, *et al.* Clinical feasibility of umbilical cord tissue-derived mesenchymal stem cells in the treatment of multiple sclerosis. *J Transl Med.* 2018;16(1):57.
- Rombouts WJ, Ploemacher RE. Primary murine MSC show highly efficient homing to the bone marrow but lose homing ability following culture. *Leukemia*. 2003 Jan;17(1):160-70.
- Ruetze M, Richter W. Adipose-derived stromal cells for osteoarticular repair: trophic function versus stem cell activity. *Expert Rev Mol Med*. 2014; 16:e9.
- Salama BF, Korbutt GS. Porcine islet xenografts: a clinical source of ß-cell grafts. *Curr Diab Rep*. 2017; 17(3): 14.

- Schuurman HJ. Regulatory aspects of clinical xenotransplantation. *Int J Surg*. 2015; 23(Pt B): 312–321.
- Scott LJ. Darvadstrocel: a review in treatment-refractory complex perianal fistulas in Crohn's disease. *BioDrugs*. 2018; 32(6): 627–634.
- Sellak H, Franzini E, Hakim J, Pasquier C. Reactive oxygen species rapidly increase endothelial ICAM-1 ability to bind neutrophils without detectable upregulation. *Blood.* 1994;83(9):2669–2677.
- Sidney LE, Branch MJ, Dunphy SE, Dua HS, Hopkinson A. Concise review: evidence for CD34 as a common marker for diverse progenitors. *Stem Cells*. 2014; 32(6): 1380–1389.
- Sordi V, Piemonti L. Mesenchymal stem cells as feeder cells for pancreatic islet transplants. *Rev Diabet Stud*. 2010; 7(2): 132–143.
- Staff NP, Jones DT, Singer W. Mesenchymal stromal cell therapies for neurodegenerative diseases. *Mayo Clin Proc*. 2019; 94(5): 892–905.
- Suga H, Eto H, Aoi N, Kato H, Araki J, Doi K, *et al.* Adipose tissue remodeling under ischemia: death of adipocytes and activation of stem/progenitor cells. *Plast Reconstr Surg.* 2010;126(6):1911–1923.
- Tachibana K. N-cadherin-mediated aggregate formation; cell detachment by Trypsin-EDTA loses N-cadherin and delays aggregate formation. *Biochem Biophys Res Comm*. 2019; 516(2):414–418.
- Tachida Y, Suda K, Nagase H, Shimada K, Isono F, Kobayashi H. Secreted factors from adipose tissue-derived mesenchymal stem cells suppress oxygen/glucose deprivation-induced cardiomyocyte cell death via furin/PCSK-like enzyme activity. *Biochem Biophys Rep*. 2016; 7: 266–272.
- Tamura A, Matsubara O. Pulmonary tumor embolism: relationship between clinical manifestations and pathologic findings. *Nihon Kyobu Shikkan Gakkai Zasshi.* 1993;31(10):1269–1278.
- Tanihara F, Hirata M, Nguyen NT, Sawamoto O, Kikuchi T, Doi M, *et al.* Efficient generation of GGTA1-deficient pigs by electroporation of the CRISPR/Cas9 system into in vitro-fertilized zygotes. *BMC Biotechnol*. 2020; 20(1): 40.
- Tanihara F, Hirata M, Nguyen NT, Sawamoto O, Kikuchi T, Otoi T. One-step generation of multiple gene-edited pigs by electroporation of the CRISPR/Cas9 system into zygotes to reduce xenoantigen biosynthesis. *Int J Mol Sci*. 2021; 22(5): 2249.
- Terashvili M, Bosnjak Z.J. Stem cell therapies in cardiovascular disease. *J Cardiothorac Vasc Anesth.* 2019;33(1):209–222.

- Thirlwell KL, Colligan D, Mountford JC, Samuel K, Bailey L, Cuesta-Gomez N, *et al.* Pancreas-derived mesenchymal stromal cells share immune response-modulating and angiogenic potential with bone marrow mesenchymal stromal cells and can be grown to therapeutic scale under Good Manufacturing Practice conditions. *Cytotherapy*. 2020; 22(12): 762–771.
- Togami W, Sei A, Okada T, Taniwaki T, Fujimoto T, Nakamura T, *et al.* Effects of water-holding capability of the PVF sponge on the adhesion and differentiation of rat bone marrow stem cell culture. *J Biomed Mater Res A.* 2014;102(1):247–253.
- Trounson A, McDonald C. Stem cell therapies in clinical trials: progress and challenges. *Cell Stem Cell.* 2015;17(1):11–22.
- Tsujimoto H, Osafune K. Current status and future directions of clinical applications using iPS cells-focus on Japan. *FEBS J*. 2022 Dec;289(23):7274-7291.
- Wang H, Strange C, Nietert PJ, Wang J, Turnbull TL, Cloud C, *et al.* Autologous mesenchymal stem cell and islet cotransplantation: safety and efficacy. *Stem Cells Transl Med*. 2018; 7(1): 11–19.
- Watanabe T, Yasuda S, Kusakawa S, Kuroda T, Futamura M, Ogawa M, *et al.* Multisite studies for validation and improvement of a highly efficient culture assay for detection of undifferentiated human pluripotent stem cells intermingled in cell therapy products. *Cytotherapy*. 2021; 23(2): 176–183.
- Wu XB, Tao R. Hepatocyte differentiation of mesenchymal stem cells. *Hepatobiliary Pancreat Dis Int*. 2012; Aug 15;11(4):360-71.
- Wuchter P, Boda-Heggemann J, Straub B.K, Grund C., Kuhn C, Krause U, *et al.* Processus and recessus adhaerentes: giant adherens cell junction systems connect and attract human mesenchymal stem cells. *Cell Tissue Res.* 2007;328(3):499–514.
- Wyles C.C, Houdek M.T, Behfar A, Sierra R.J. Mesenchymal stem cell therapy for osteoarthritis: current perspectives. *Stem Cells Cloning.* 2015;8:117–124.
- Yamada H, Naito R, Nishimura M, Kawakami R, Morinaga E, Morita Y, *et al.* Xenotransplantation of neonatal porcine bone marrow-derived mesenchymal stem cells improves diabetic wound healing by promoting angiogenesis and lymphangiogenesis. *Xenotransplantation*. 2022; 29(2):e12739.
- Yamada H, Sakata N, Nishimura M, Tanaka T, Shimizu M, Yoshimatsu G, *et al.* Xenotransplantation of neonatal porcine bone marrow-derived mesenchymal stem cells improves murine hind limb ischemia through lymphangiogenesis and angiogenesis. *Xenotransplantation*. 2021; 28(4):e12693.
- Yamanaka S. Pluripotent Stem Cell-Based Cell Therapy-Promise and Challenges. *Cell Stem Cell*. 2020 Oct 1;27(4):523-531.

- Yang YK, Ogando CR, Wang See C, Chang TY, Barabino GA. Changes in phenotype and differentiation potential of human mesenchymal stem cells aging in vitro. *Stem Cell Res Ther*. 2018; 9(1): 131.
- Yaykasli KO, Schauer C, Muñoz LE, Mahajan A, Knopf J, Schett G, Herrmann M. Neutrophil extracellular trap-driven occlusive diseases. *Cells.* 2021. 10(9):2208.
- Yin D, Ding J.W, Shen J, Ma L, Hara M, Chong A.S. Liver ischemia contributes to early islet failure following intraportal transplantation: benefits of liver ischemic-preconditioning. *Am J Transplant.* 2006;6(1):60–68.
- Yokota N, Hattori M, Ohtsuru T, Otsuji M, Lyman S, Shimomura K, *et al.* Comparative clinical outcomes after intra-articular injection with adipose-derived cultured stem cells or noncultured stromal vascular fraction for the treatment of knee osteoarthritis. *Am J Sports Med*. 2019; 47(11): 2577–2583.
- Zhan L, Rao JS, Sethia N, Slama MQ, Han Z, Tobolt D, *et al.* Pancreatic islet cryopreservation by vitrification achieves high viability, function, recovery and clinical scalability for transplantation. *Nat Med*. 2022; 28(4): 798–808.
- Zhang Y, Fan N, Yang J. Expression and clinical significance of hypoxia-inducible factor 1α, Snail and E-cadherin in human ovarian cancer cell lines. *Mol Med Rep.* 2015;12(3):3393–3399.
- Zou J, Yang W, Cui W, Li C, Ma C, Ji X, *et al*. Therapeutic potential and mechanisms of mesenchymal stem cell-derived exosomes as bioactive materials in tendon-bone healing. *J Nanobiotechnology*. 2023; Jan 16;21(1):14.